

N66-14065

(ACCESSION NUMBER)

(THRU)

(PAGES)

(CODE)

(NASA CR OR TMX OR AD NUMBER)

(CATEGORY)

NASA CR-54787
LAC ER- 8231

GPO PRICE \$

CFSTI PRICE(S) \$

Hard copy (HC) 3.00

Microfiche (MF) -75

ff 653 July 65



EFFECT OF NUCLEAR RADIATION ON MATERIALS AT CRYOGENIC TEMPERATURES

by

LOCKHEED NUCLEAR PRODUCTS

C. A. Schwanbeck, Project Manager

prepared for

NATIONAL AERONAUTICS AND SPACE ADMINISTRATION

Contract NAS3-7985

LOCKHEED NUCLEAR PRODUCTS

NOTICE

This report was prepared as an account of Government sponsored work. Neither the United States, nor the National Aeronautics and Space Administration (NASA), nor any person acting on behalf of NASA:

- A.) Makes any warranty or representation, expressed or implied, with respect to the accuracy, completeness, or usefulness of the information contained in this report, or that the use of any information, apparatus, method, or process disclosed in this report may not infringe privately owned rights; or
- B.) Assumes any liabilities with respect to the use of, or for damages resulting from the use of any information, apparatus, method or process disclosed in this report.

As used above, "person acting on behalf of NASA" includes any employee or contractor of NASA, or employee of such contractor, to the extent that such employee or contractor of NASA, or employee of such contractor prepares, disseminates, or provides access to, any information pursuant to his employment or contract with NASA, or his employment with such contractor.

Requests for copies of this report should be referred to

National Aeronautics and Space Administration
Office of Scientific and Technical Information
Attention: AFSS-A
Washington, D.C. 20546

QUARTERLY REPORT NO. 1

July 21, 1965 Through October 21, 1965

EFFECT OF NUCLEAR RADIATION ON MATERIALS
AT CRYOGENIC TEMPERATURES

by

LOCKHEED NUCLEAR PRODUCTS

C. A. Schwanbeck, Project Manager

prepared for

NATIONAL AERONAUTICS AND SPACE ADMINISTRATION

November 1965

Contract NAS 3-7985

Technical Management
NASA Lewis Research Center
Cleveland, Ohio
Nuclear Reactor Division
Charles L. Younger

LOCKHEED NUCLEAR PRODUCTS
LOCKHEED-GEORGIA COMPANY

A DIVISION OF LOCKHEED AIRCRAFT CORPORATION

If this document is supplied under the requirements of a United States Government contract, the following legend shall apply unless the letter U appears in the coding box:

This data is furnished under a United States Government contract and only those portions hereof which are marked (for example, by circling, underscoring or otherwise) and indicated as being subject to this legend shall not be released outside the Government (except to foreign governments, subject to these same limitations), nor be disclosed, used, or duplicated, for procurement or manufacturing purposes, except as otherwise authorized by contract, without the permission of Lockheed-Georgia Company, A Division of Lockheed Aircraft Corporation, Marietta, Georgia. This legend shall be marked on any reproduction hereon in whole or in part.

The "otherwise marking" and "indicated portions" as used above shall mean this statement and includes all details or manufacture contained herein respectively.

Code: U Contract: NAS 3-7985

F O R E W O R D

This quarterly report is submitted to the National Aeronautics and Space Administration, Lewis Research Center, by the Lockheed-Georgia Company in accordance with the requirements of NASA Contract NAS 3-7985.

TABLE OF CONTENTS

Section	Page
Foreword	iii
Table of Contents	v
List of Figures	vii
List of Tables	ix
1 Summary	1
2 Introduction	3
3 Test Equipment	7
3.1 Identification	7
3.2 Test Loops	9
3.3 Refrigeration System	23
3.4 Load Control System	26
3.5 Transfer System	37
3.6 Sample Change Equipment	41
3.7 Miscellaneous Test Equipment	44
3.8 Test Equipment Maintenance and Calibration	44
3.9 Experiment Design Manual and Hazards Analysis	55
4 Test Procedures	57
4.1 Test Specimen Design and Fabrication	57
4.2 Flux Mapping	61
4.3 Tensile Test Methods	61
4.4 Fatigue Test Methods	72
4.5 Structural Studies	73
5 Test Program	75
5.1 Materials Selection	75
5.2 Scope	76
Appendix A - Distribution	81

LIST OF FIGURES

Figure		Page
1	System Layout	8
2	Test Equipment (Block Diagram)	10
3	Tension And Compression Test Loop	12
4	Welding Fixture For Welding The Blank-Off Cup Into The Nuclear Instrumentation Tube	14
5	Test Loop Head Assembly With Blank-Off Cup	15
6	Tensile Test Loop Assembly	19
7	Structural Member Modification	21
8	Schematic Diagram of Refrigeration System	24
9	Calorimetric Refrigeration Capacity With Respect To Gas Temperature	27
10	Tensile Load Control System (Block Diagram)	29
11	Fatigue Load Control System (Block Diagram)	31
12	Oil Pressure To Water Pressure Conversion System	34
13	Electrical Cycle Control Schematic Preliminary Load Control System	35
14	Hydraulic Panel Cycle Control Schematic Preliminary Load Control System	36
15	Test Loop Transfer System	39
16	Hot Cave	42
17	Cask	45
18	Equipment Operation Typical Irradiation Test Cycle Vs. Hrs.	47
19	Expansion Engine Maintenance Schedule	48
20	Test Facility Equipment Maintenance Schedule	50
21	Test Loop Head Assembly Cask	53
22	Thermocouple Installation in Test Loop	64
23	Platinum Resistance Thermometer and Instrumented Specimen Calibration Arrangement	65
24	Thermocouple Calibration Curve	66
25	Thermocouple Correction Factors	67
26	Instrumented Specimen In Holders	68

LIST OF TABLES

Table		Page
1	Tensile Test Program (Scope)	77
2	Fatigue Test Program (Scope)	78

1 SUMMARY

This is the first quarterly progress report on Contract NAS 3-7985, entitled, "The Effect of Nuclear Radiation on Materials at Cryogenic Temperatures."

The scope of the test program is divided into two general phases, tensile testing and low-cycle fatigue testing. The tensile testing phase will utilize existing test loops and includes a study of the effects of irradiation at 30°R to 10^{18} nvt, a study of the effects of irradiation temperature, and a study of the effects of self-annealing following irradiation. The low-cycle fatigue testing phase requires extensive modification of existing test loops and the hydraulic load control system and includes both fatigue testing during irradiation at 30°R and fatigue testing following irradiation at 30°R to 10^{17} nvt.

Author

The materials selected for study were based on the need for engineering data at higher flux levels than heretofore attained at cryogenic temperatures, and on the need for more fundamental data on the mechanical properties of metals under neutron irradiation at cryogenic temperatures. Titanium and several titanium alloys and alloy conditions have been selected for the engineering studies and Aluminum 1099 has been selected for fundamental as well as engineering studies.

Progress during this reporting period has been in the form of necessary preparations and modification of existing test loops and equipment with no actual test results to date.

The test specimens for the tensile testing phase of the test program have been fabricated, but fabrication of the fatigue specimens will be postponed pending final specimen design.

Test loop modification for low-cycle fatigue testing has required considerable effort devoted to the development and design of a method for reinforcing the test loop structural member for improved alignment under loading and improved fatigue resistance. Also, a method for removing one of the two seals (between the refrigerated helium and the cooling water) in the test loop head assemblies was developed and has been employed in modification of three unirradiated head assemblies.

The existing hydraulic load control system is being completely revamped to facilitate the low cycle fatigue testing with a controlled shape to the stress versus time cycle. The required modifications have been established and the system has been ordered for delivery before the end of January 1966. A preliminary load control

system without the refinements of the final system is being constructed for the purpose of qualifying the modified test loops and the fatigue specimen design before delivery of the permanent system.

During performance of maintenance and calibration of test equipment and instrumentation, a number of leaks were detected in the test loops. These leaks have been, or are in the process of being, repaired.

A new beam port gamma shield was installed in the reactor facility during this reporting period. Realignment of the transfer system and adjustments to facilitate inserting the test loop an additional 0.25", which is permitted by the internal dimensions of the new shield, have been completed. However, before actual test results can be obtained, neutron flux mapping and temperature correlation measurements are required. Procedures for these measurements have been initiated but were not complete at the end of this reporting period.

2 INTRODUCTION

The combination of a fast neutron and cryogenic environment encountered in the structural members of a liquid hydrogen nuclear rocket imposes service conditions dissimilar to those encountered in other engineering applications. Both fast neutron bombardment and extremely low temperatures affect the mechanical properties of engineering materials; therefore the magnitude of the combined effect must be determined to provide basic design information before materials for a reliable nuclear rocket system can be selected. Since the neutron irradiation effects are self-healing through spontaneous annealing even at low temperatures, tests to provide the desired information concerning the combined effect must be conducted with the specimens held at the temperature of interest during the entire irradiation and testing period.

A screening program (reference 1) was undertaken to assess the effect of fast neutron irradiation on selected engineering alloys at temperatures near the boiling point of liquid hydrogen (-423°F). Tensile tests on parallel sample sets of unnotched specimens for each alloy at room temperature unirradiated; at 30°R (-430°F) unirradiated and at 30°R irradiated to $1 \times 10^{17} \text{ n/cm}^2$ (energies greater than 0.5 Mev) were performed at the NASA Plum Brook Reactor Facility using a helium refrigerator and testing equipment specially designed for in-pile testing under controlled temperature conditions.

Test results from the screening program indicated that titanium alloys possessed the highest strength-to-weight ratio following exposure to the combined nuclear-cryogenic environment as well as being among the least susceptible to deterioration of mechanical properties of the alloys tested. On the other hand, Aluminum 1099 (99.99% Aluminum) was found to be very sensitive to both irradiation and temperature of irradiation.

Based on the information obtained from the screening program, an in-pile test program (see Section 5) has been initiated to study in greater detail the effects of a combined nuclear-cryogenic environment on the mechanical properties of metals. The objective of this program is to provide engineering data at higher flux levels and/or under different load conditions than heretofore attained at cryogenic temperatures as well as data for more fundamental studies. Its scope consists of two general phases, tensile testing and low-cycle fatigue testing. The tensile testing phase includes irradiations at 30°R to 10^{18} n/cm^2 ($E > 0.5 \text{ Mev}$),

(1). Quarterly Progress Reports 1-16, Contract NASw-114.

irradiations to 10^{17} n/cm² ($E > 0.5$ Mev) at temperatures between 30°R and room temperature (540°R), and irradiations to 10^{17} n/cm² ($E > 0.5$ Mev) at 30°R followed by specimen warm-up prior to fracture. The low-cycle fatigue testing phase includes both fatigue testing during irradiation at 30°R and fatigue testing following irradiation at 30°R to 10^{17} n/cm² ($E > 0.5$ Mev).

Existing test equipment (see Section 3) will be utilized during performance of the test program. Most of this equipment has recently undergone major overhaul and modification (reference 2) in preparation for the nominal 140 hour test period to obtain 10^{18} n/cm² ($E > 0.5$ Mev) exposures. Maintenance and calibration schedules, established during this overhaul effort, should keep the equipment operating reliably.

The tensile testing phase of the test program will precede the fatigue testing phase due to extensive modification of test loops and the hydraulic load control system necessary for cyclic loading. A qualification procedure will be conducted to demonstrate the adequacy of the test equipment for the tensile testing phase of the program as well as to give some additional data points. This qualification is required because of the organic seals which are used in the test loops to isolate the static helium refrigerant, under pressure in the head assembly, from the cooling water. These seals have operated satisfactorily to 10^{17} nvt ($E > 0.5$ Mev) irradiations but there is not assurance that they will retain their sealing characteristics after irradiations to 10^{18} nvt. Tests to 3×10^{17} nvt and 6×10^{17} nvt at 30°R will be performed before undertaking the experiments which are to require 10^{18} nvt.

As in the screening program (reference 1), standard test specimens cannot be used in this test program due to various restrictions on the test equipment imposed by the nuclear cryogenic environment. The tensile specimens to be used represent a miniaturization of the standard ASTM E-8 specimen (reference 3). Although fatigue specimen design is not as standardized as tensile specimen design, the fatigue specimens used in this program will be miniature and will represent a departure from any commonly used design.

A newly designed and fabricated gamma shield has been installed in the Plum Brook Reactor HB-2 beam port irradiation facility. This change requires new calibrations (see Section 4), including neutron flux mapping and temperature correlations.

-
- (2). Summary Report, NASA CR-54770.
 - (1). Quarterly Progress Reports 1-16, Contract NASw-114.
 - (3). Anon: ASTM Standards, The American Society for Testing Materials, 1958, Part 3, pp 103-119.

Progress during this first quarter of Contract NAS 3-7985 has been in the form of necessary preparations and modifications of existing test loops with no actual test results to date. Pertinent information is reported in the following sections.

3 TEST EQUIPMENT

3.1 IDENTIFICATION

The test equipment for in-pile and out-of-pile testing under controlled temperature and load conditions permits the test program to be performed wholly by remote operations. Major components of the test equipment and the test operation can be readily identified and followed by reference to Figure 1.

The irradiated specimens to be tested during this program will require protracted - up to about 140 hours - exposures in a high flux zone of the NASA Plum Brook 60 MW (th) nuclear reactor with the specimen maintained at a specific temperature. The irradiations are to be conducted in a test location adjacent to the beryllium reflector on the north face of the reactor core. Access to this zone is through a 9 inch ID horizontal beam port (HB-2) located approximately 20 feet below the surface of a pool of demineralized water which provides biological shielding during reactor operations. The beam port, which penetrates a high density concrete biological shield two feet thick, the reactor pressure vessel and the reactor thermal shield, is approximately six and one-half feet in length from its external flange to the high flux test zone. However, the full ID of HB-2 is not available as a test zone since a gamma shield, required to permit specimen temperature control at 30°R with refrigeration capacity of 1150 watts, limits the internal diameter of the beam port to 6 inches.

For tensile test performance, a test loop is inserted into the hot cave for specimen installation. After completion of loop re-assembly following specimen insertion, the loop is withdrawn from the hot cave to the north table in Quadrant "D". Refrigerant flow is started and the table holding the loop is rotated 180°. The loop is then transferred to the south table and positioned in line with HB-2 and, after stabilization of specimen temperature at the temperature to be maintained throughout the test, inserted into HB-2.

The loop is held in this position with the specimen maintained at temperature until the accumulated fast neutron dose is attained. At this time, an axial tensile load is applied to the specimen and increased until failure occurs.

After specimen failure, the loop is returned to the hot cave for specimen replacement.

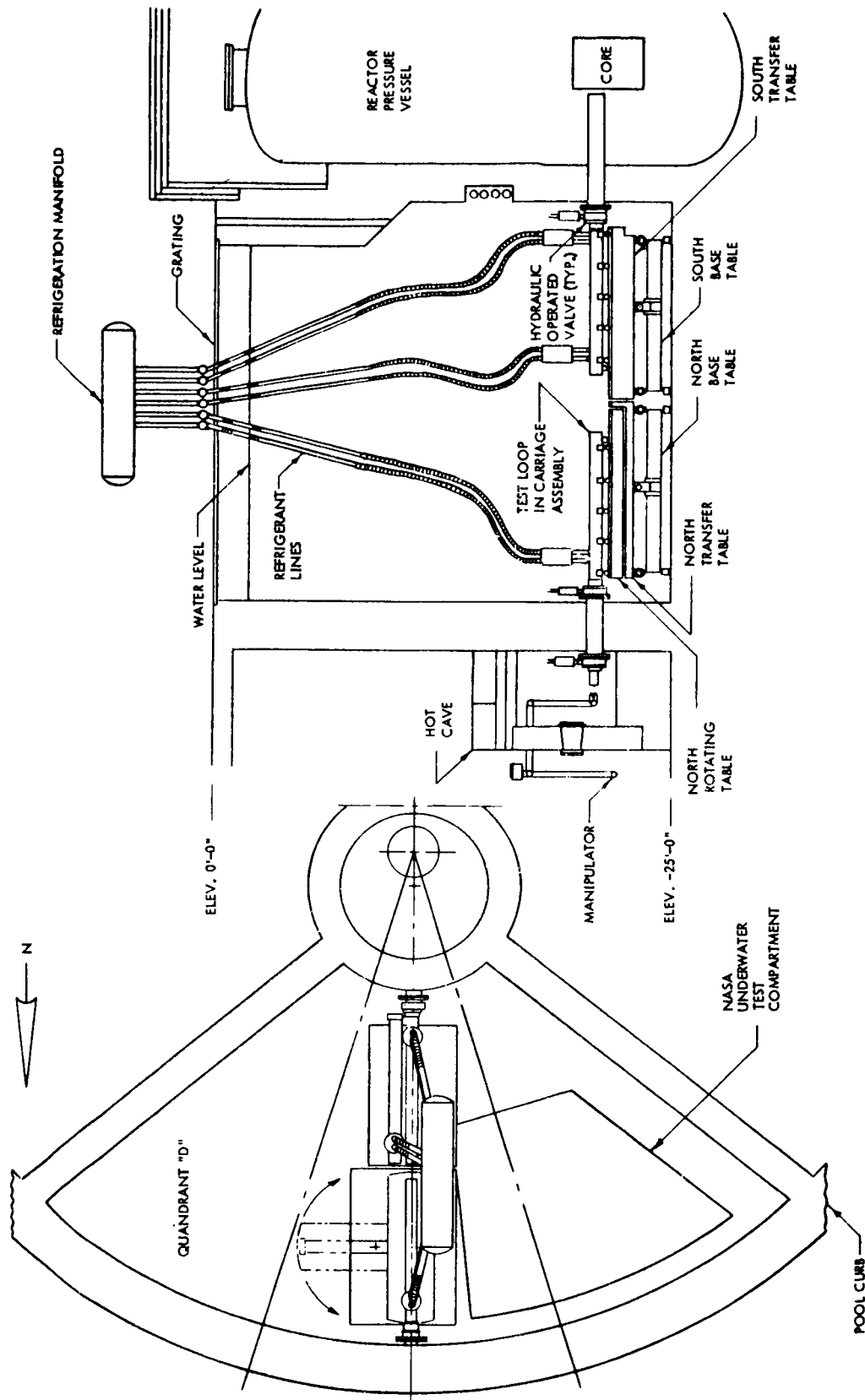


FIGURE 1 SYSTEM LAYOUT

During operation, two test loops are normally used for alternate insertion in HB-2, thus providing a maximum utilization of reactor operating time. While one loop is undergoing irradiation, the second loop is undergoing specimen replacement and cool-down operations. The system also has provisions for using three test loops simultaneously with proper allocation of refrigerant.

The requirements of the present test program, particularly the low-cycle fatigue testing, necessitates much preliminary effort in the form of analysis and modifications of the test equipment. Although this equipment is highly specialized, it may be conveniently separated into the six categories shown in Figure 2 for discussions of design, modification, and maintenance efforts, as well as performance characteristics during test program operation.

3.2 TEST LOOPS

The test loops currently available are stainless steel cylindrical envelopes, 6 inches OD by about 9 feet long, containing all necessary equipment for irradiating a test specimen under precise temperature control conditions and fracturing the specimen, at temperature, in tension or compression without removal from the irradiation field. At the aft end of the test loop; fittings are provided for tying in the refrigeration system, the load control system, and the instrumentation and data recording system. Other fittings are provided for test loop cooling using deionized water (which must be isolated from the helium).

These test loops will be used to perform the tensile test program and, after modification, the low-cycle fatigue test program.

3.2.1 Tensile Test Loops

Five tensile test loops are currently available for use in performing the test program. These loops are designated as 201-001, 201-002, 201-003, 201-004, and 201-005. Test loop 201-001 is a prototype and cannot be used in-pile. Test loops 201-002, 201-003, and 201-004 were used during a previously conducted in-pile test program and are, therefore, radioactive. Test loop 201-005 has not yet been placed in service.

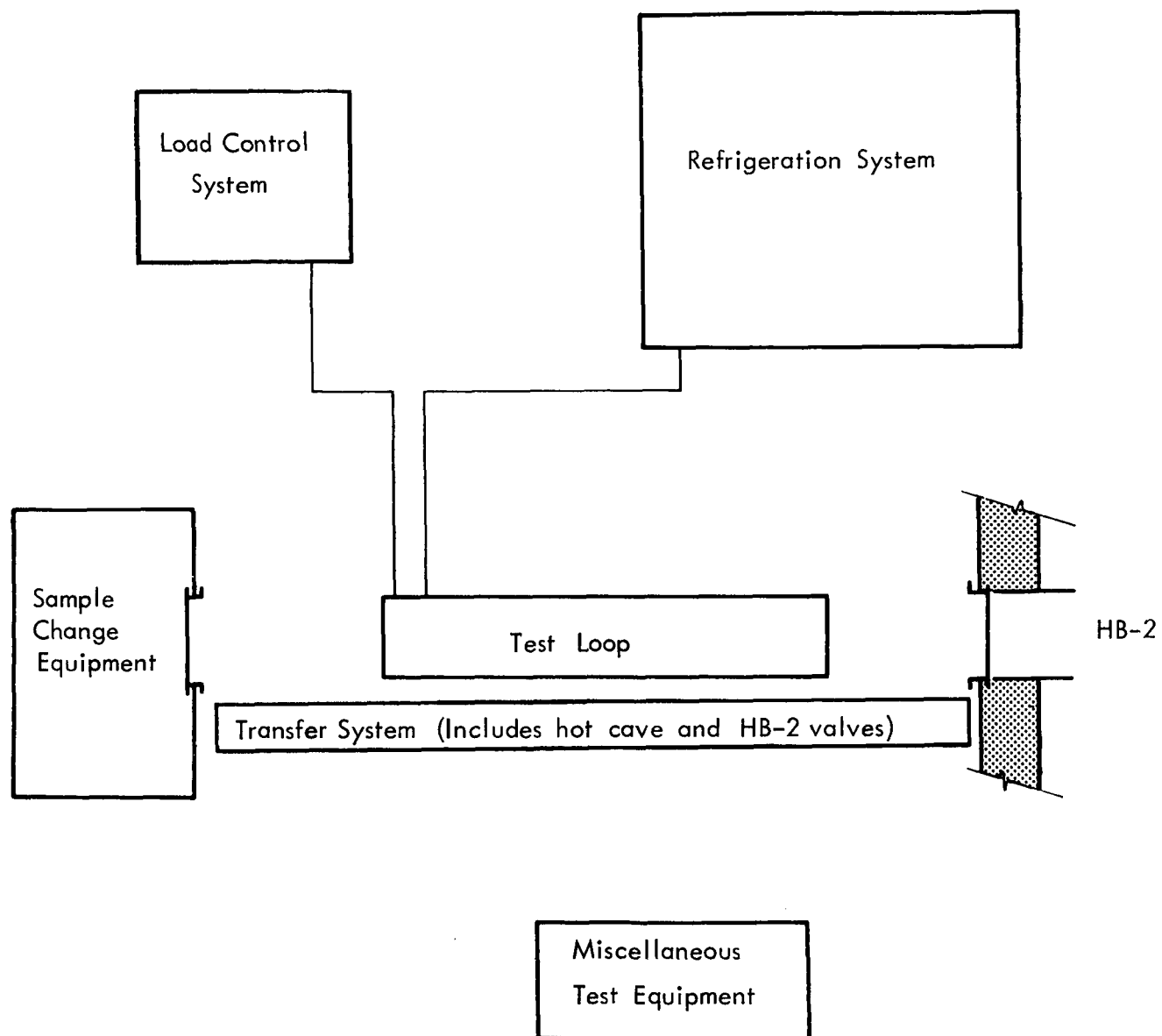


FIGURE 2 TEST EQUIPMENT (BLOCK DIAGRAM)

Head assemblies 201-007 and 201-008, however, have leaks in their bellows assemblies and head assembly 201-010 has a hole in the nuclear instrumentation tube (see Section 3.2.1.2.1) so that these three heads cannot be used until repairs are effected.

3.2.1.1 Design

The tension-compression test loops currently available are specially designed envelopes containing a horizontally placed 5000 pound capacity tensile testing machine together with the requisite stress-strain monitoring instrumentation and vacuum insulated refrigerant transfer lines in a 6 inch OD tubular housing of sufficient length to place the test specimen in the high neutron flux zone. The design features of these test loops are shown in Figure 3.

The tensile testing machine is actuated by a hydraulic cylinder using demineralized water as the working fluid to avoid the possible contamination of reactor primary or quadrant water with other fluids. The force is transmitted to the specimen through a push rod guided by two self-aligning graphite bearings. The load cell consists of a ring type dynamometer equipped with a linear variable differential transformer. The output of the LVDT is a function of the deflection in the ring which, in turn, is a measure of the applied load. The forward section, or head, of the test loop is removable to allow specimen change by remote handling methods. The holders on both forward and aft ends of the test specimen are assembled using mating spherical seats to insure proper alignment during application of the test load. Helium guides direct the refrigerant over the specimen in a flow pattern which assures adequate specimen temperature control.

3.2.1.2 Modification

3.2.1.2.1 Nuclear Instrumentation Seal Elimination

The test loops originally incorporated nuclear instrumentation in the head assembly which proved to be impractical and was abandoned early in the screening program. The tube for this instrumentation remains and is internally cooled with circulating

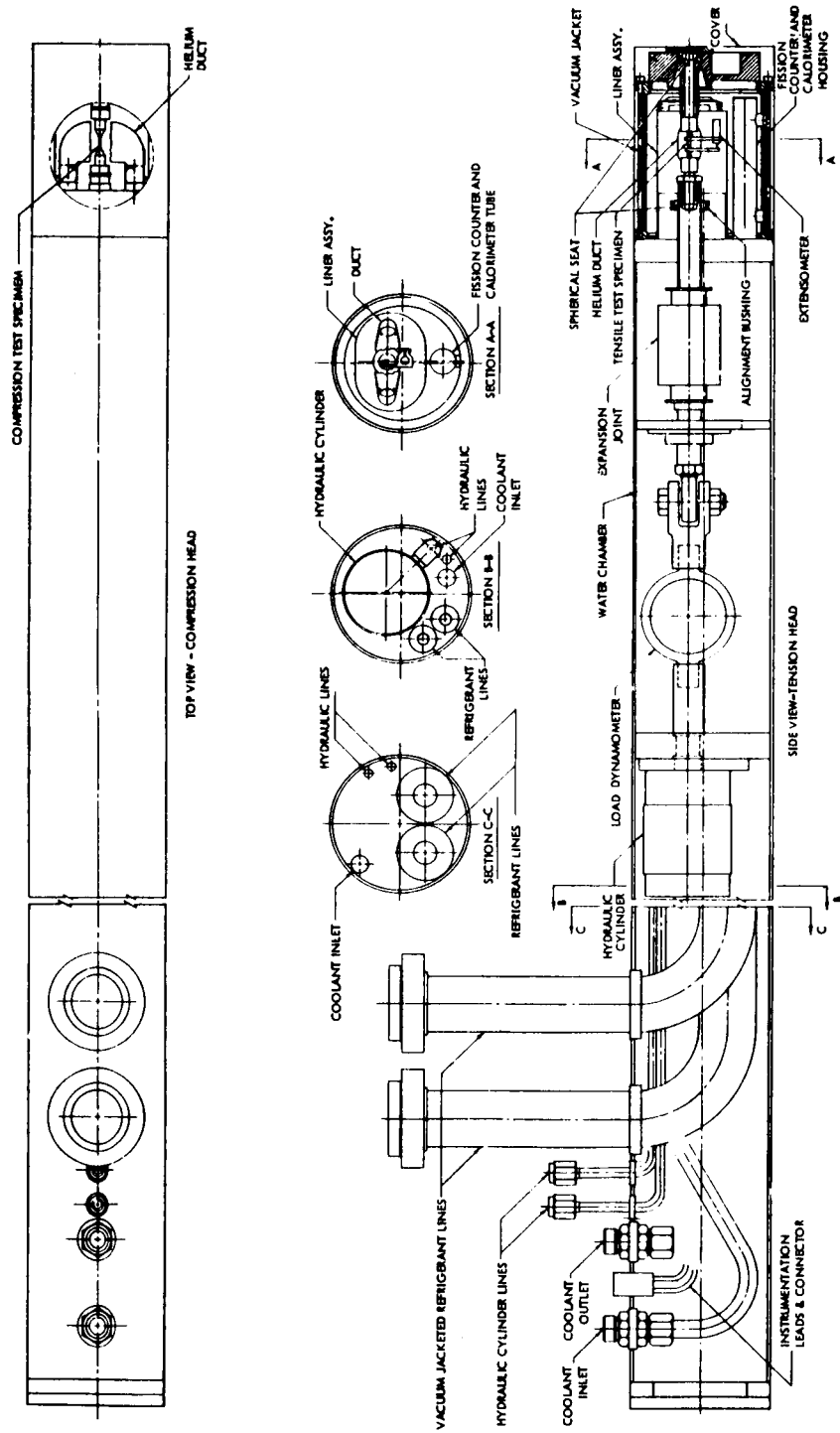


FIGURE 3 TENSION AND COMPRESSION TEST LOOP

water which has to be isolated from the helium refrigerant at the test loop bulkhead with an "O" ring type seal. This instrumentation tube seal is a source of difficulty because of helium leakage into the quadrant water when the test loop is withdrawn from the reactor beam port after a test. Also, since it is mechanically in parallel with an outer seal which isolates other head assembly cooling water from the refrigerant, it detracts from the effectiveness of the outer seal. This seal will be eliminated by welding a blank off cap into the instrumentation tube.

During this reporting period, a fixture (see Figure 4) was fabricated for remotely welding the blank off caps into the position indicated in Figure 5. Since this fixture was designed with the center of rotation to be coincident with the center line of the nuclear instrumentation tube, a mock-up of a head assembly was also fabricated. Provisions were made in this mock-up to permit replacement of the tubes in which the blank-off cups were to be welded. Numerous tests on mock-up components were conducted to develop welding parameters and techniques. A prime consideration of the operation of blanking off this tube was the effect of the vacuum surrounding the tube on the structural integrity of the tube at welding temperature. Tests indicated that it would be more feasible to perform the work with an ambient environment so the vacuum would be vented to atmosphere in all head assemblies before proceeding with welding of the cap into the head.

The fixture has been utilized for welding unirradiated head assemblies 201-006, 201-009, and 201-011. After welding, these three assemblies were first checked with a helium mass spectrometer at ambient conditions for (1) possible burn-through of the tube in the welding process which would introduce a leak into the vacuum and (2) the integrity of the weld to assure that water in the remainder of the tube could not enter the helium cavity. Subsequently, they were leak tested at 400°F, evacuated and sealed. All heads indicate, by a low liquid nitrogen boil off rate, a successful seal weld and are, therefore, considered complete in the new configuration.

Attempts to weld the blank off cup in irradiated test loop head assemblies have thus far been unsuccessful. The cup was placed in the nuclear instrumentation tube of test loop head assembly 201-010 and the remote weld was initiated. During the traverse of the electrode, however, it was noted that the weld was not continuous. The operation was stopped and the fixture and electrode holder were checked for alignment. The second try did not produce appreciably better results, so the fixture was removed from the hot cave and checked for alignment and tested for ability to perform satisfactory welds. It was then replaced in the hot cave and another attempt made with no appreciably better results. By this time, though, there was distinct evidence

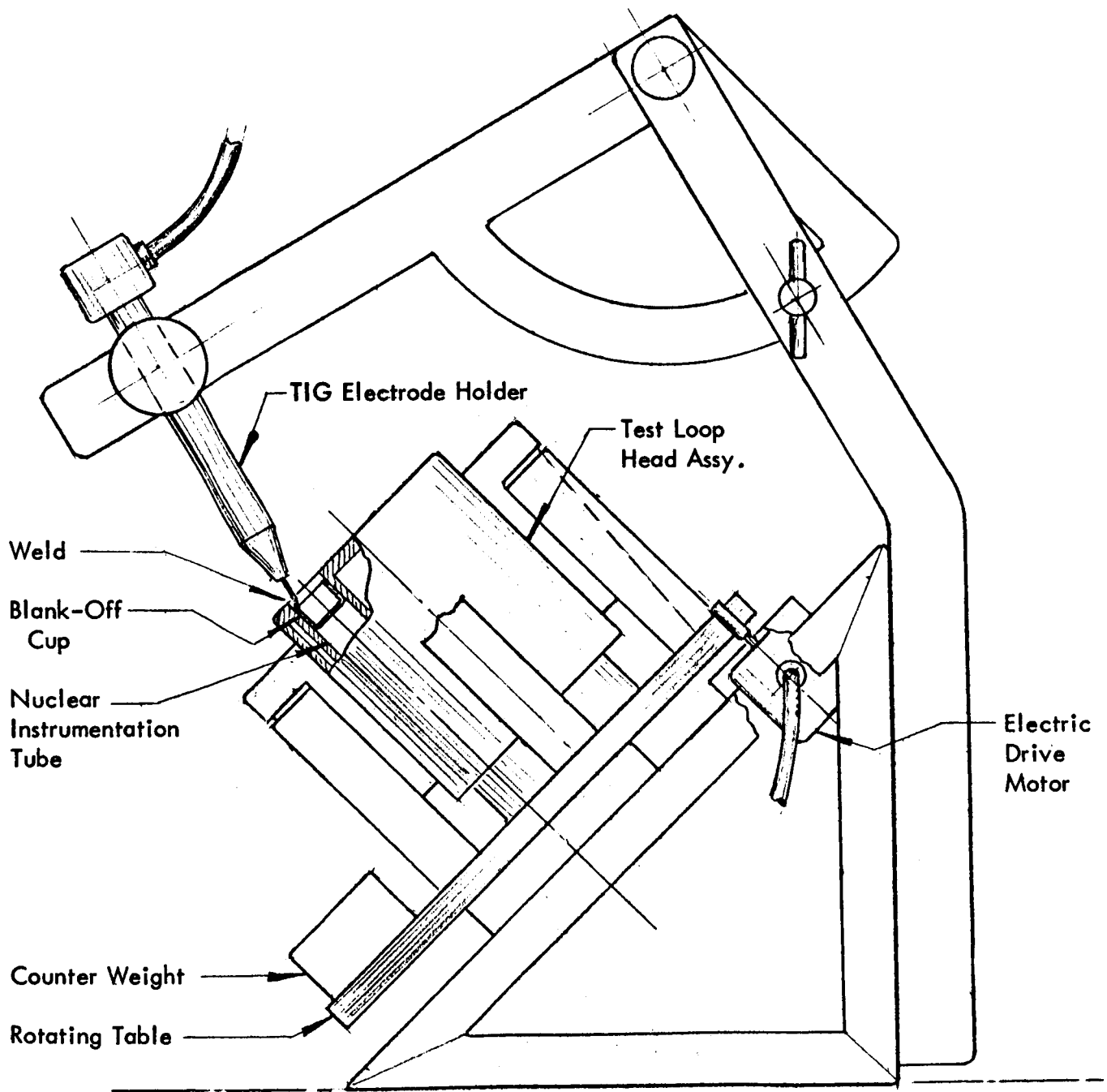


FIGURE 4 WELDING FIXTURE FOR WELDING THE BLANK-OFF CUP INTO THE NUCLEAR INSTRUMENTATION TUBE

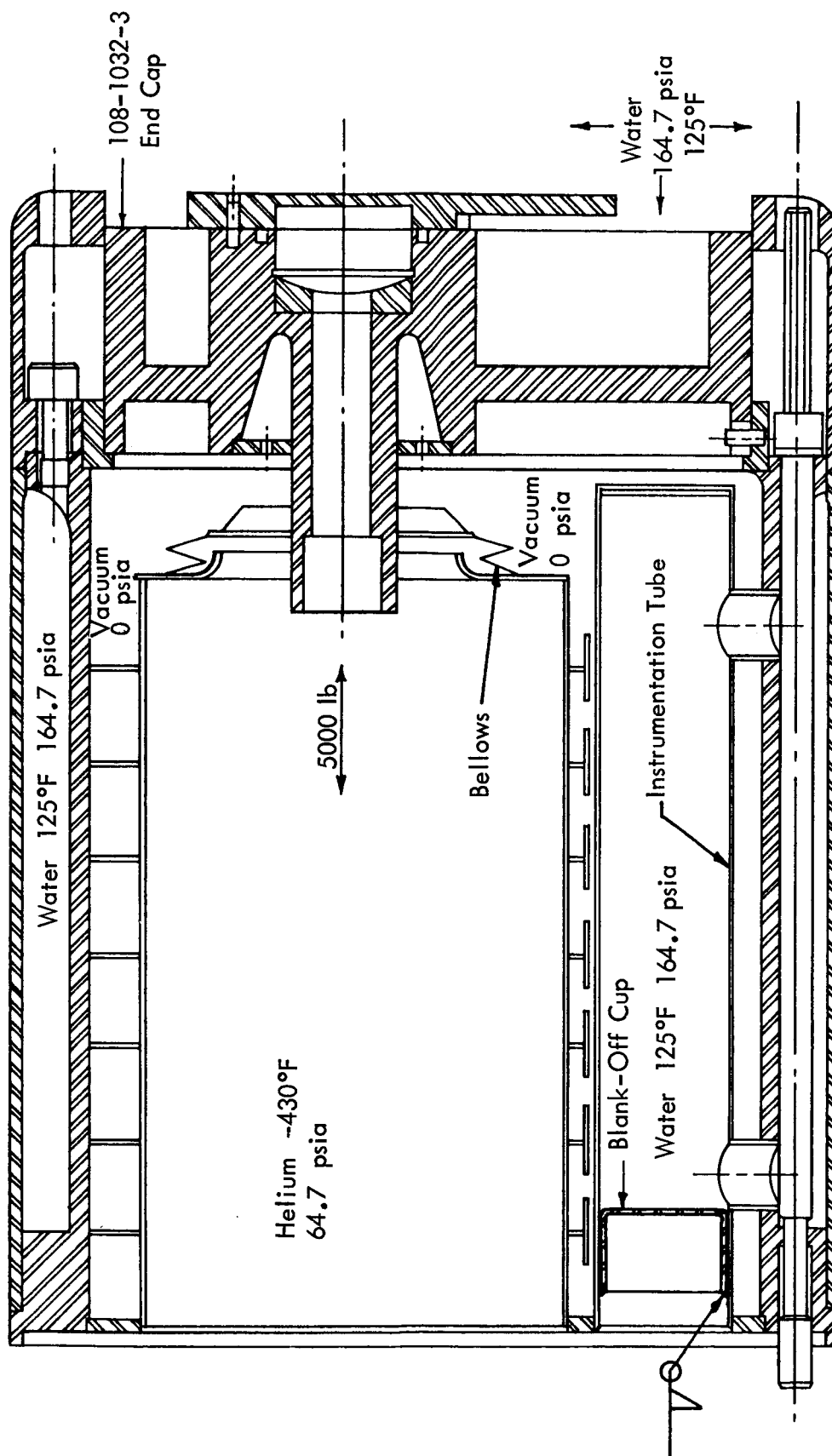


FIGURE 5 TEST LOOP HEAD ASSEMBLY WITH BLANK-OFF CUP

of clearance between the cup and the nuclear instrumentation tube due to warpage from the amount of heat involved in the weld attempts. In addition, the lip of the blank off cup was distorted and uneven. In an attempt to circumvent the problem of trying to position the electrode over an uneven surface, it was decided to attempt to hold the electrode with a manipulator and do the welding manually. Checks for welding current settings were performed and dry runs were made to determine if such a method was feasible. The operation was started and a weld bead was made approximately halfway around the cup but the clearance between the cup and tube kept increasing. Attempts were made to add material to fill the gap but before sufficient material could be added, a hole in the nuclear instrumentation tube developed, thus causing a cessation of activity on this head assembly. The decision was then made to further check the welding fixture to determine the cause for the malfunction before further welding was performed.

3.2.1.3 Performance

3.2.1.3.1 Test Loops

The prototype test loop (201-001) will be used for determining the design and modification requirements for low-cycle fatigue testing. Further discussions pertaining to this test loop are presented in Section 3.2.2.1.

Test loop 201-005 will be retained in the unirradiated condition and will be modified later for low-cycle fatigue testing. Further discussions pertaining to this test loop are presented in Section 3.2.2.2.

It was initially planned to use test loops 201-002 and 201-004 for the tensile test program since loop 201-003 was the least radioactive of the three. However, leaks were detected in the test loops (see Section 3.9.2.1) and loop 201-003 will be used for the tensile test program. One of these three loops will be modified for low-cycle fatigue testing subsequent to procedure development and modification of loop 201-005.

Test loop performance during this reporting period relative to the test program is summarized as follows:

- (1) Test loop 201-002 was not used due to leaks which are yet to be repaired.

- (2) Test loop 201-003 has been prepared for initial flux mapping and subsequent tensile testing.
- (3) Test loop 201-004 was used successfully for out-of-pile temperature correlations and will be used for forthcoming in-pile temperature correlations.

3.2.1.3.2 Test Loop Head Assemblies

The three irradiated head assemblies (201-007, 201-008, and 201-010) are currently not available for use in the in-pile test program due to various leaks which have not yet been repaired (see sections 3.2.1.2.1 and 3.8.2.2). This requires placing into service the three unirradiated head assemblies.

Test loop head assembly performance during this reporting period relative to the test program is summarized as follows:

- (1) Head assembly 201-007 not available due to leaks which must be repaired.
- (2) Head assembly 201-008 not available due to leaks which must be repaired.
- (3) Head assembly 201-010 not available due to leaks which must be repaired.
- (4) Head assembly 201-006 installed on test loop 201-004.
- (5) Head assembly 201-009 on stand-by ready for use.
- (6) Head assembly 201-011 installed on test loop 201-003.

3.2.1.3.3 Qualification of Test Loop Head Assembly Organic Seals

The requirements for specimen change in the test loop are met with the removable head technique. This requires the use of seals to isolate the static helium refrigerant, under pressure in the head assembly, from the cooling water. Organic seals are currently being used for this application and have performed satisfactorily

for 10^{17} n/cm² ($E > 0.5$ Mev) irradiations, but there is no assurance that they will retain their sealing characteristics for 10^{18} n/cm² ($E > 0.5$ Mev) irradiations.

An investigation, commencing with reactor cycle 39P, will be conducted to qualify these seals for the longer tests in-pile. Seals will be qualified by actual service, first for 3×10^{17} n/cm², then for 6×10^{17} n/cm², and finally for 10^{18} n/cm².

3.2.2 Fatigue Test Loops

Low-cycle, axial tension-compression fatigue tests are to be performed using existing tension-compression test loops. The original specifications to which the existing test loops were built required that they be capable of exerting tensile or compressive loads, but not both in a cyclic manner. These test loops will require considerable analysis and modification before reliable test data can be obtained. Preliminary analysis of the alignment requirements indicate that good specimen alignment will be necessary to yield interpretable test results. The existing self-aligning features in the loading linkage must therefore be eliminated.

3.2.2.1 Design

An experimental determination of the alignment of load application both in tension and compression has been initiated using the prototype tensile test loop (201-001) without the self-aligning features. The major components of the test loop under consideration are shown in Figure 6.

3.2.2.1.1 Structural Member

The structural member installed in the test loop, as shown in Figure 6, acts as a column directing the loads that occur during insertion into the carriage trunnion and is also the assembly which supports the specimen loading actuator. The load applied in the test specimen is transmitted through the head assembly back through this member to the actuator. The load resulting from testing is distributed peripherally and transmitted eccentrically into the member. During a preliminary determination of the alignment problem, loads were applied by the actuator to this assembly and a peripheral displacement was measured. The maximum displacement occurred at 4.37 inches aft of the forward mounting flange and was 0.019 inch at 4400 pounds.

Shown in Expanded Section Below

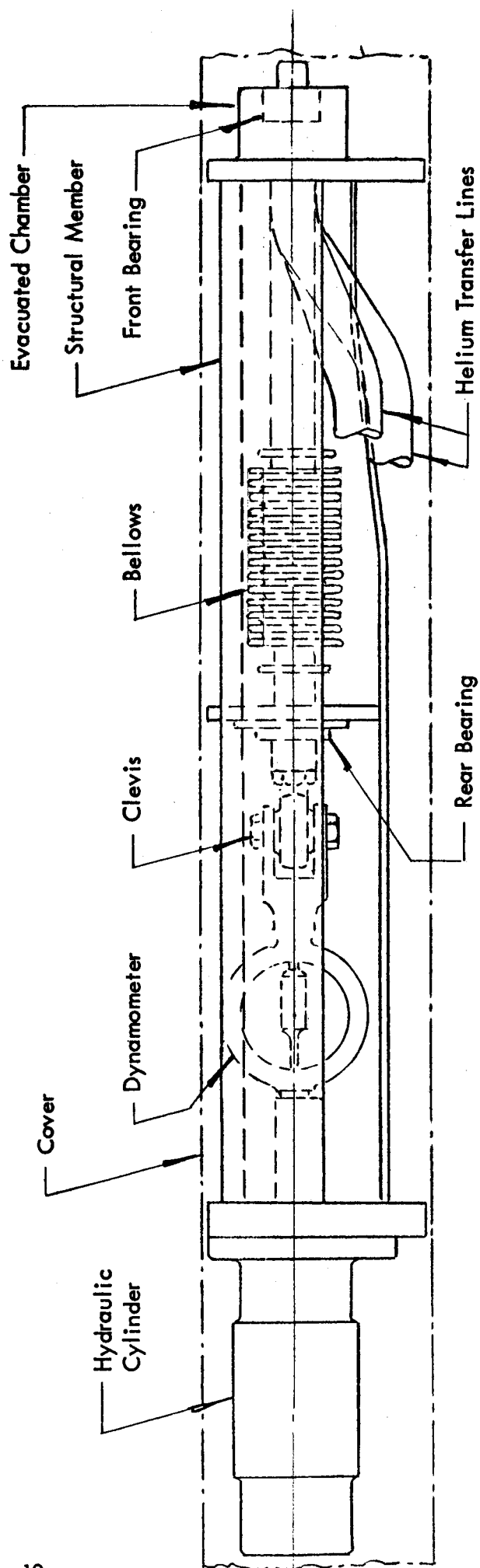
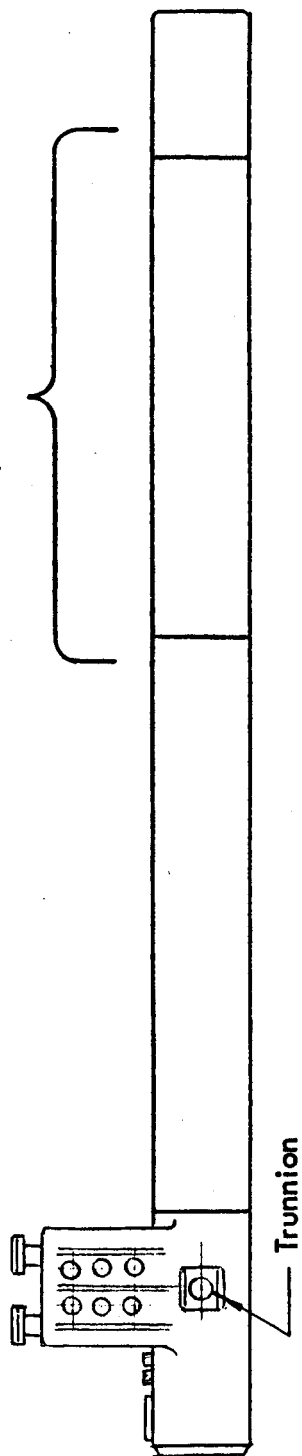


FIGURE 6 TENSILE TEST LOOP ASSEMBLY

To reduce this deflection, various concepts for stay braces were developed and templates were fabricated to establish installation feasibility. The concepts incorporating greater inherent stiffness could not be used due to interferences with the helium refrigerant line and instrumentation tubes. As a consequence the segmented assembly as shown in Figure 7 was developed and installed. After installation the member was again loaded and maximum peripheral displacement of 0.006 inch at 5000 pound load occurred 2.0 inches aft of the forward end.

Additional changes will be made in an effort to reduce this distortion as much as possible as well as to determine the magnitude of misalignment in the loading linkage as a result of the elimination of the self-aligning features.

3.2.2.1.2 Lost Motion in Pull Rod Linkage

The lost motion in the pull rod linkage in the test loop was necessary information to assist in determining the hydraulic power supply capacity required for the fatigue testing. This was measured at two different loads as indicated below:

Load on Dynamometer	Movement of Cylinder Rod	Movement at Front of Dynamometer Ring	Movement at Front of Eye Bolt
3500#	.090"	.058"	.038"
1000#	.030"	.022"	.010"

3.2.2.1.3 Hydraulic Actuator Seals

During cycling with a preliminary control system (see section 3.4), the "O" ring type seals in the hydraulic actuator of the prototype test loop started to fail initially after 1800 cycles and were replaced at about 2000 cycles. An undetermined amount of wear had occurred previously in these seals since nearly all of the out-of-pile portion of a previous test program was performed using this cylinder. Over 1400 cycles have now been made on the cylinder with new seals. The load during most of these cycles has been 3500 and 4400 pounds on the dynamometer. The maximum anticipated load during the fatigue testing program is less than 3500 pounds, but the seals will be subjected to 10,000 cycles. Further testing will be performed to qualify the seals for the test program.

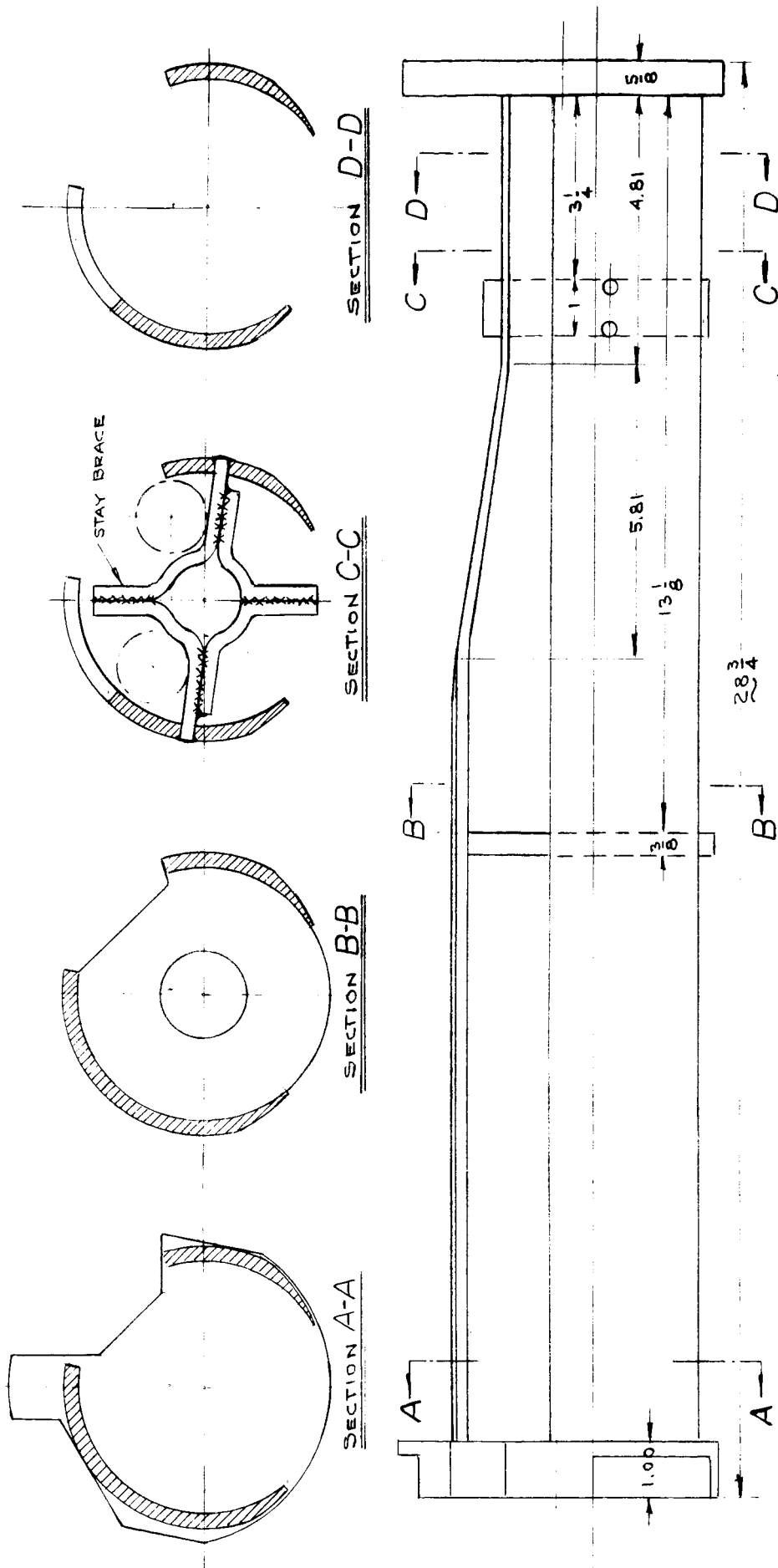


FIGURE 7 STRUCTURAL MEMBER MODIFICATION

3.2.2.2 Modification

After completion of the fatigue test loop modification requirements and detail design (section 3.2.2.1), it is planned to modify tensile test loop 201-005. During this modification, procedures will be developed for similar modification of one of the radioactive tensile test loops.

3.3 REFRIGERATION SYSTEM

Test location temperature control is provided by a closed cycle helium refrigerator with an electrically driven positive displacement compressor, a counter-flow heat exchanger and four reciprocating expansion engines. The refrigeration system was designed and built for this application and was warranted to be capable of maintaining any temperature between 30°R and room temperature in the test location of the test loops. The refrigeration system has a rated capacity of 1150 watts with a manifold temperature of 30°R.

3.3.1 Design

A schematic of the refrigeration system is shown in Figure 8. Low pressure (approximately 50 psia) helium gas is drawn into the suction side of a two stage positive displacement compressor and compressed to 300 psia. The heat of compression is removed by water cooling after each compression stage. The helium gas at 300 psia and 540°R passes through an extended surface counter flow aluminum heat exchanger capable of a 600 lb/hr flow with a duty rating of 410,000 BTU/hr. With the refrigeration system operating at 30°R, the helium gas leaves the high pressure side of the heat exchanger at approximately 37°R and 296 psia. The cold gas enters the expansion engines where it is expanded to 53 psia. These engines are coupled in pairs to crossheads which drive oil pumps which absorb work from the system to allow adiabatic gas expansion. The design specifications for the expansion engines are given below:

Mass Flow (Total)	520 lb/hr
Inlet Temperature	37°R
Outlet Temperature	24°R
Piston Displacement	7.93 ft ³ /min
Engine Speed	340 RPM

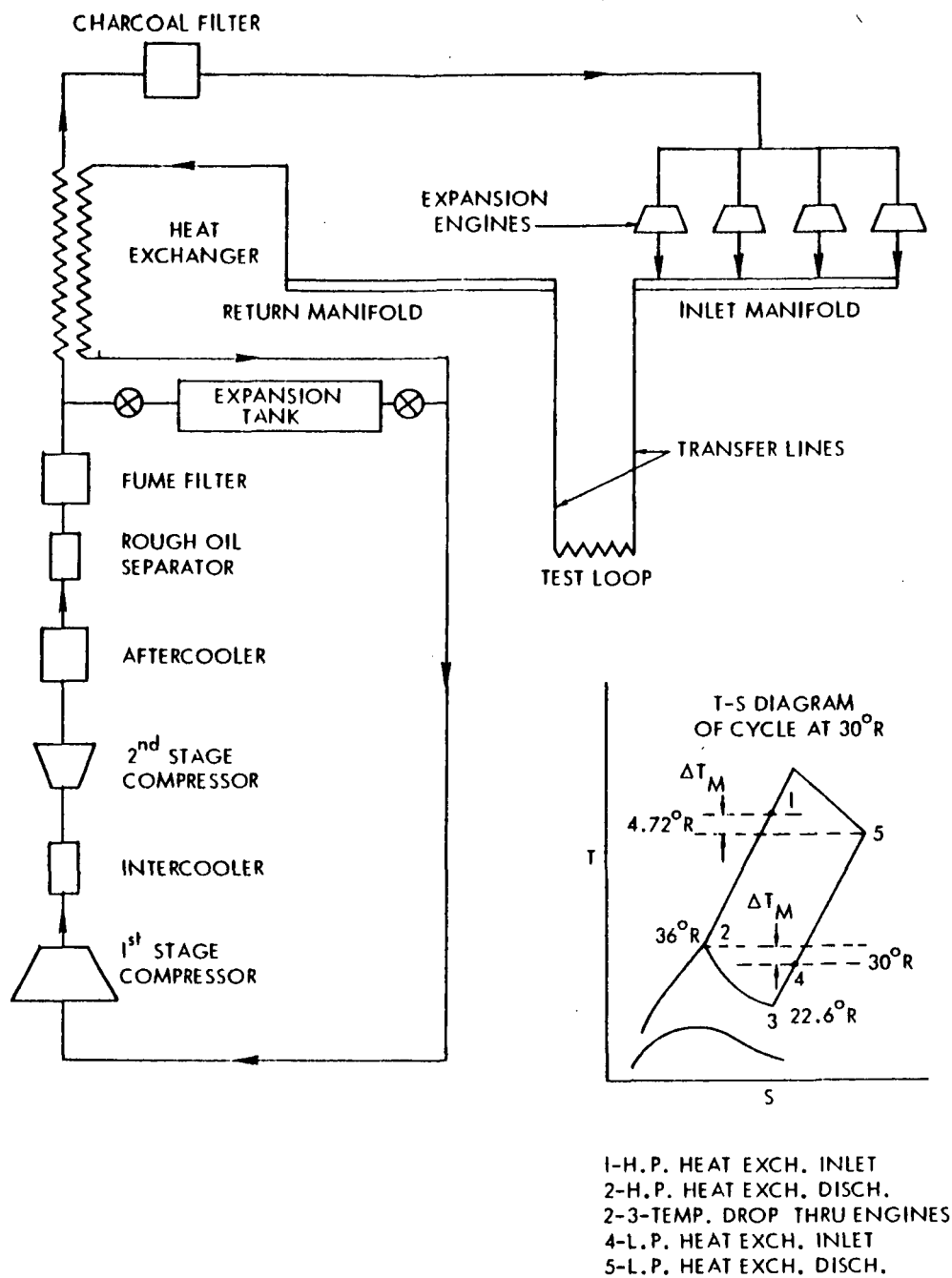


FIGURE 8 SCHEMATIC DIAGRAM OF REFRIGERATION SYSTEM

The heat exchanger and each pair of expansion engines are mounted in evacuated shells filled with powdered perlite to provide insulation.

The refrigerated gas leaving the expansion engines is transferred through vacuum insulated flexible lines to the test location in the tensile-compression test loop. After passing through the test chamber, the gas is returned through a manifold to the low pressure side of the heat exchanger and then back to the compressor suction side. A line heater of 2500 watt capacity is located in the inlet manifold and a 100 watt trim heater is located in the manifold at the inlet of each set of transfer lines to allow operation of the system at any temperature between 30°R and room temperature.

3.3.2 Modification

The refrigeration system was recently overhauled (reference 2) during which time minor modifications were made to increase system performance and reliability for long term tests.

Although no additional modifications to the refrigeration system are presently planned, one problem area does exist. One set of the helium transfer lines has sustained a leak in the flexible section of the line. This leak is from the inner bellows-like tube into the evacuated volume and is of such magnitude that the heat leak through the lines is much greater than the allowable 100 watts. This pair of lines is useless in the in-pile operation because the leak reduces the available refrigeration capacity for a test loop. In addition to this malfunction none of the valves in the valve chest assembly which are used for isolation of the test loop from the transfer lines operate properly; thus, operation of the manual extension valves in the refrigerator manifold is necessary to reduce the gas flow through the test loop. This tends to warm the transfer lines as well as the test loop during a specimen changing operation, requiring additional refrigeration capacity and time to cool a test loop after a specimen is changed. A modification to the valves in this valve chest assembly allowing them to seal better as well as making them more accessible for valve repair would reduce turn-around time between specimen changes and naturally increase the beam-port utilization factor.

3.3.3 Performance

During the major overhaul period (reference 2), the refrigeration system was tested to establish its capacity at various temperature levels. The tests were performed by installing

(2). Summary Report, NASA CR-54770.

a calorimeter which consisted of a thermally isolated electrical resistance heater in place of the test loop. With this type of installation, the heat leak from the transfer lines and calorimeter enclosure can be determined and the available refrigeration for removal of the heat leak in the test loop and gamma heating can be established by measuring the wattage of the calorimeter heater while maintaining a constant return manifold temperature.

The results of the tests which were performed at 30°R, 150°R, and 340°R at the return manifold indicate that 900 watts, 2135 watts, and 2325 watts respectively were available at the conditions of the test.

These conditions were nominal testing conditions which would approximate those used in performing actual nuclear-cryogenic tests. The ΔT measured at the test loop sensors was 4.4°R, 10.7°R and 38.2°R when refrigerating at 30°R, 150°R, and 340°R, respectively.

This increase was anticipated after determining the mass flow characteristics of the system. It is also recognized that this ΔT can be reduced by judicious application of system controllable heater loads thereby reducing the ΔT at the test specimen.

In addition, a test to determine the characteristics of the system at 540°R was performed indicating that the system can be used at this level, with difficulty, to dissipate gamma heating loads. The actual values are not shown because the system was operated with only two expansion engines and at a low rpm which provided a result which does not appear compatible with the other data; however, the 1005 watts measured is reasonable if the conditions are related to the nominal operating characteristics.

The results of the tests are shown in Figure 9 as determined by using theoretical heat exchanger requirements and previously measured transfer line heat leak.

3.4 LOAD CONTROL SYSTEM

The existing load control system for the tensile test loops is an electro-hydraulic system using demineralized water as the working fluid. The hydraulic power supply and the instrumentation and data recording components are located in the quadrant and on the grating at the 0 foot level. The test loops, in turn, have permanently installed components and instrumentation (a hydraulic cylinder, dynamometer, and extensometer lead lines) which are included as part of the load control system.

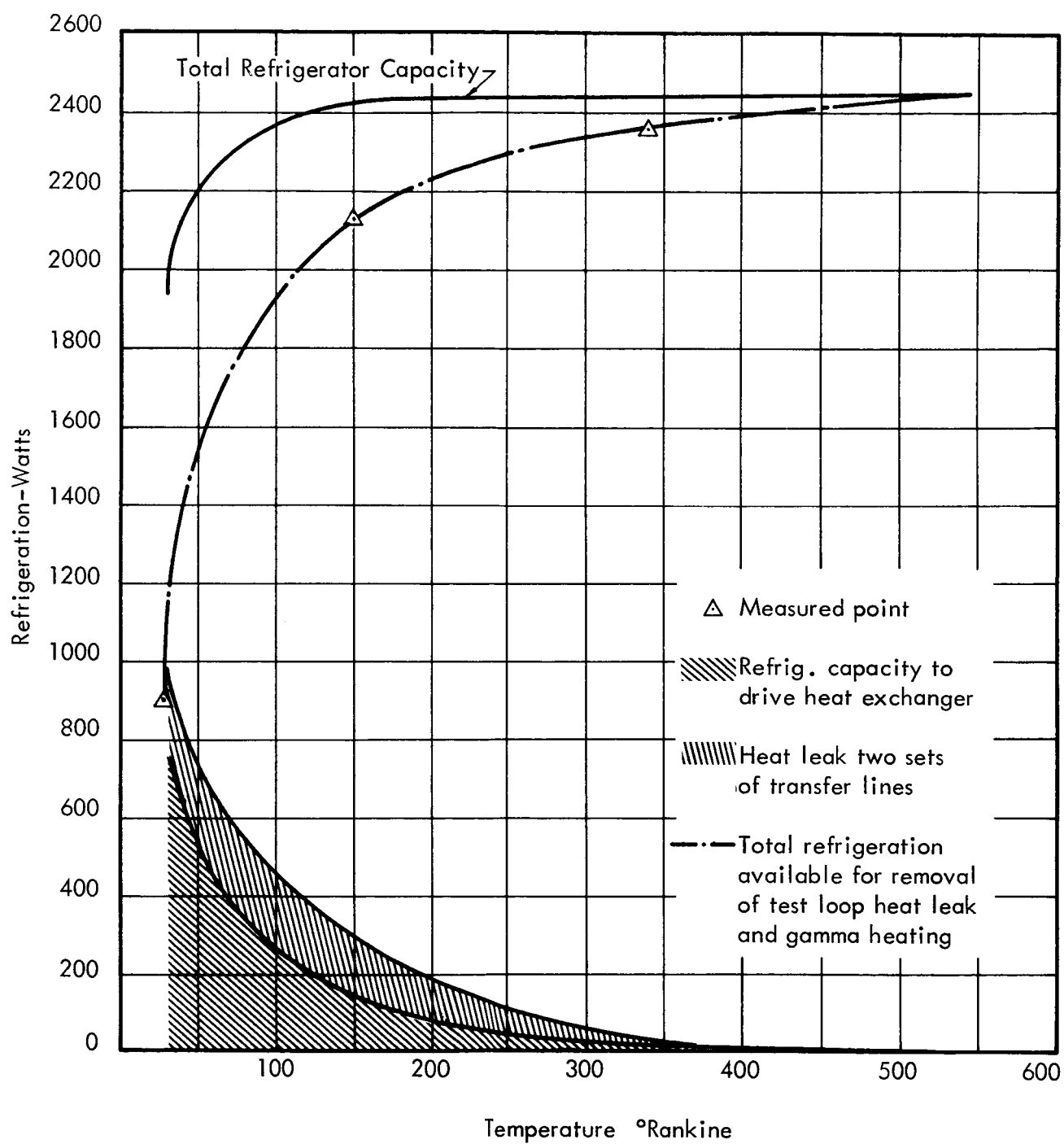


FIGURE 9 CALORIMETRIC REFRIGERATION CAPACITY WITH RESPECT TO GAS TEMPERATURE

3.4.1 Tensile Test Loop Load Control System

3.4.1.1 Design

A schematic of the tensile test loop load control system is shown in Figure 10.

3.4.1.2 Modification

Major modification of control system is anticipated and this modification is to be described in detail in section 3.4.2.

3.4.1.3 Performance

No serious difficulties have been encountered with the existing control system during tensile type testing over a period of several years.

3.4.2 Fatigue Test Loop Load Control System

The low-cycle fatigue testing requires that the existing load control system be completely revamped. The high applied stress levels (up to 90% of the ultimate tensile strength) of the tests require special regard to accuracy of measurement and control of the applied load. There is also the requirement of a cyclic rate which is variable from 5 cpm up to the limitation of the system. Other requirements include the ability to maintain constant cyclic rate, the ability to stop a test automatically on failure of the specimen, a means for measuring maximum and minimum tensile and/or compressive stress, and means for indicating the number of cycles. Also, a sinusoidal, or nearly sinusoidal, stress versus time load must be applied to the specimen to reduce impact-type effects and to reduce the variables of the experiment. Another requirement is that the maximum stress in a given cycle be programmed in such a way as to minimize the chance for buckling under compressive loading and again to reduce the variables of the experiment. These requirements dictate the required pumping capacity of the fatigue actuator hydraulic supply system.

3.4.2.1 Design

A closed loop electro-hydraulic servo system will be used to meet the fatigue test loop

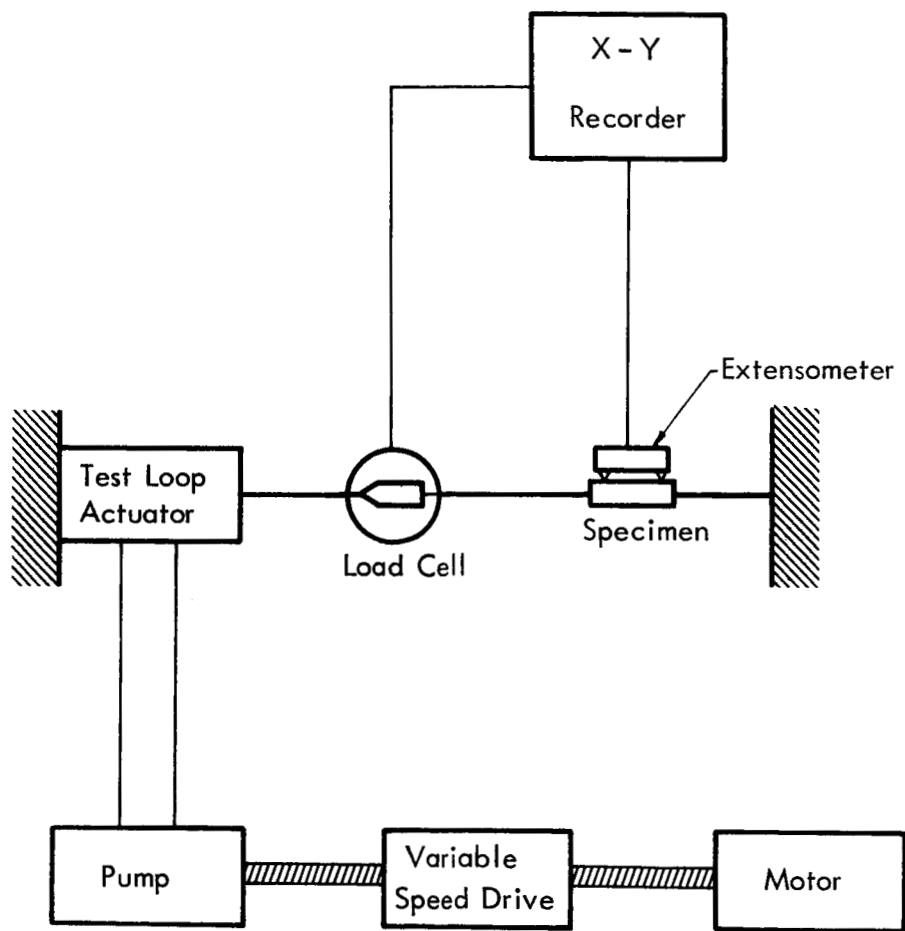


FIGURE 10 TENSILE LOAD CONTROL SYSTEM (BLOCK DIAGRAM)

control system requirements. The servo approach can be relied on to meet the requirements more reliably and more economically than any other approach and at the same time to provide a high quality universal testing system, applicable to tensile testing as well as fatigue testing.

Equipment is available commercially for this approach and the buckling under compressive loading can be minimized by increasing the amplitude of the load versus time plot linearly over approximately 100 cycles at the beginning of the cyclic loading. A schematic of the system is shown in Figure 11.

The complete system has many inherent features and capabilities which are not essential to meet the present requirements. Some of these are completely contained while others would require minor modifications or added modules. System changes will not be required to convert from a static tensile tester to a fatigue tester or vice-versa. Only the command signal will require consideration which is a matter of electrical selection. For tensile testing with load control, a linearly increasing command will allow the test to be performed at constant rate of load application. Loading rate will be proportional to the slope of the linear command and this slope will be variable. Modular additions in the command circuit will allow loading functions other than linear to be utilized. By attaching an extensometer to the test section of the specimen and using the extensometer for feed-back, the tensile tests can be performed at constant strain rate. Change in strain rate can be accomplished in the same manner previously described for changing load rate. Relatively high rates are possible with the proposed system.

As described above for tensile testing, fatigue tests could also be performed with either load control or strain control with the addition of a suitable strain transducer on the test specimen. Consequently, fatigue testing could be performed at constant strain amplitude while recording change in load amplitude. Conversely strain amplitudes could be recorded while testing at constant load amplitudes. Also, there is infinite variability of load or strain ratio. With the function generator specified, the load form can be selected as sinusoidal, square or sawtooth. All components are capable of high response with potential for cyclic rates in excess of twenty-five cycles per second. Modular additions will allow random, or ordered spectral type loading or straining.

The fact that the test loop actually must be operated with deionized water rather than a petroleum-base hydraulic fluid to avoid possible contamination of the reactor primary coolant water complicates the requirements in that a hydraulic servo control system made from stock components cannot function reliably with water. This means that a two-fluid system must be used. Even though the operational principal is the

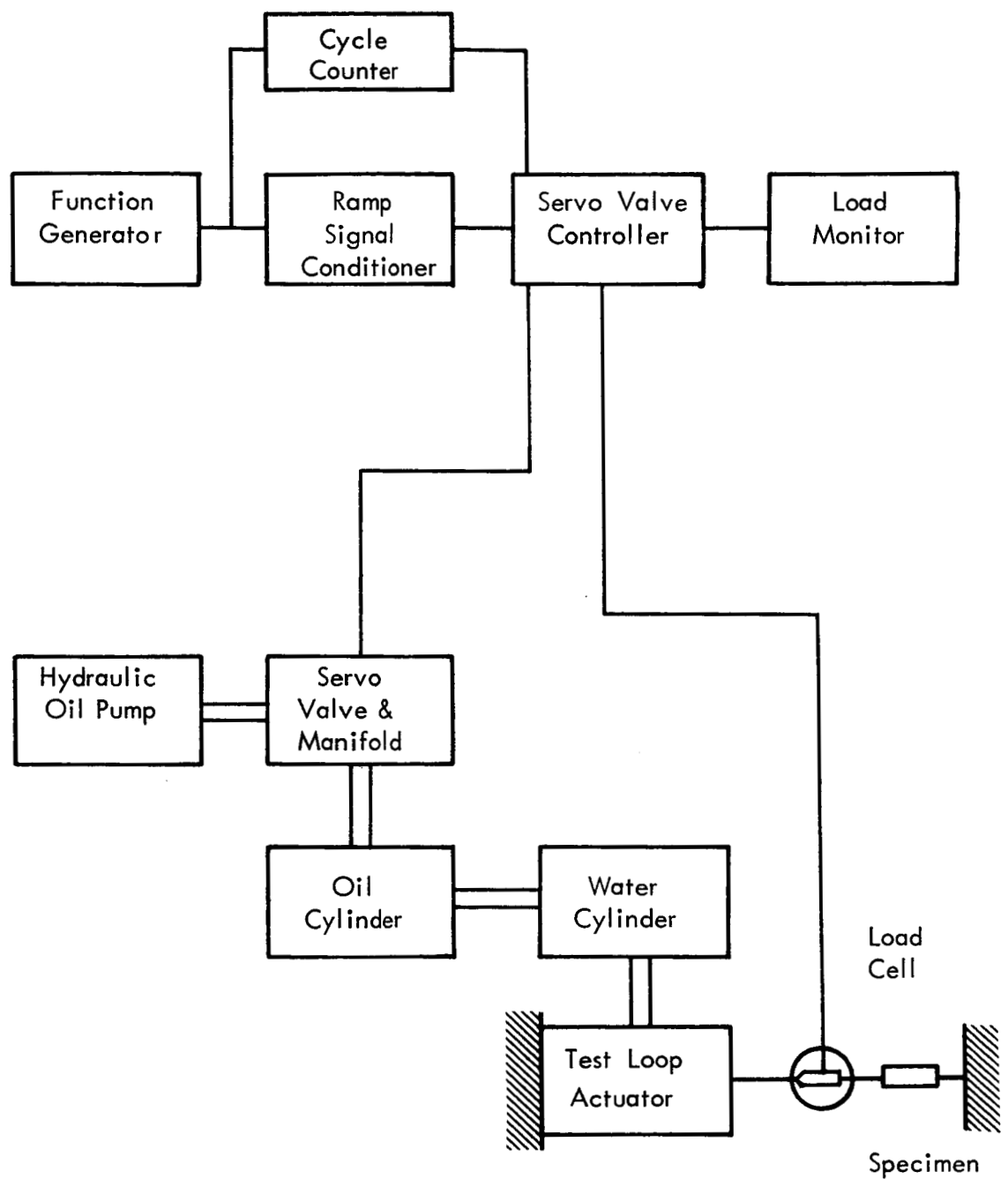


FIGURE 11 FATIGUE LOAD CONTROL SYSTEM (BLOCK DIAGRAM)

same as that described herein there are complexities which result from the need for fail safe controls, and a two-fluid hydraulic system. These two necessities impose the most rigid, and possibly the most difficult requirements, of the whole equipment modification.

An electrical command signal proportional to the desired specimen load is applied at the summing junction. Since as yet there is no feed back signal at the summing junction, the entire command signal is amplified by the servo amplifier. The amplified signal, in turn, displaces the electro-hydraulic servo valve spool which allows fluid to enter the actuator and apply load to the specimen. A feed back signal is then generated by a transducer contained in the load cell. This feed back is summed with the command which reduces the signal to the servo amplifier. Once the load proportional to the command signal is reached, the servo amplifier signal has vanished and the desired load is maintained until the command is changed. If, instead of a steady command, a varying command is induced, the specimen will be subjected to proportional load variations.

Input demand signal to the system will be from a low frequency function generator. This generator will give an output sinusoidal wave variable in frequency over a range of .01 cps to 1000 cps. Other wave shapes (square and triangular) are also available by switch setting.

A signal conditioning circuit is provided which will allow the output amplitude of the function generator to be linearly controlled by a ramp function to a pre-calculated value. The ramp function will be employed at the beginning of each test and will continue for 100 cycles at which time the desired constant load amplitude will be reached and maintained for the test duration. Such signal conditioning will be provided to standardize test start procedures and thus minimize uncontrolled variables such as initial misalignment or buckling of the test specimen application of the load. An over-ride switch will be provided on the Signal Conditioner to permit system set-up and operation when the linear varying amplitude input (ramp) signal is not required.

A servo valve controller equipped with a differential transformer conditioning module will be utilized. The conditioning module permits both feed back control and load monitoring to be accomplished using the signal from a single differential transformer. Consequently, changes in the existing load cell (dynamometer) are not required.

The controller has error detectors which actuate warning lights and fail safe by-pass valves which either dump pressure or lock the system when the specimen fails. The error detector also protects the specimen from overload in the event of system malfunction inasmuch as by-pass valves are opened as a function of error voltage magnitude.

The error detector voltage will be additionally employed to de-energize an electro-magnetic counter which will count the command signal and, hence, the number of load cycles applied to the specimen. Upon specimen failure, error voltage magnitude will actuate a latching relay which interrupts the power to the electro-magnetic counter. The counter retains the total number of cycles accomplished prior to failure.

In addition to error detectors and feed back signal conditioning, the servo controller is composed of additional electronic circuitry in the form of an error amplifier, valve amplifier, demodulator and stability network.

The servo valve works directly with the servo controller and is a pilot-operated closed center, four-way sliding spool valve in which the output flow to a constant load is proportional to electrical input current. It will operate with normal petroleum base hydraulic oil, the supply of which will be furnished by a new hydraulic power supply.

The oil actuator will be of the double-ended type which operates with petroleum base hydraulic fluid. It will mechanically couple with the shaft of a second actuator, operating with water, and of the type in the existing test loops. This arrangement furnishes water pressure to the test loop actuator and eliminates the possibility of contaminating the primary coolant water, as shown in Figure 12. Motion of the oil actuator forces the water actuator piston to move and this motion is transmitted hydraulically to the test loop actuator. Each of the water lines will be connected to the water source through a check valve and a pressure regulator valve. Water leakage losses will be made up on the low pressure side of the test loop actuator, alternately each half cycle.

The test loop actuator is the actuator that applies a load to the specimen. The dynamometer is connected mechanically in series with the actuator rod and the specimen. This device is the feed back component used to null the demand signal. It is also employed to monitor the load excursions.

The control system purchase order has been let for delivery by the end of January 1966. Upon delivery, the system will be installed in the reactor containment vessel.

The magnitude of the changes required to convert a tensile test loop into a low cyclic rate fatigue type of test loop was not fully known at the initiation of the program. Therefore, it was decided to assemble a preliminary control system as shown in Figures 13 and 14, capable of exerting alternate tensile and compressive loads on test specimens. This system is not servo controlled and therefore does not apply the load in the proposed sinusoidal manner but is still capable of providing information concerning test loop modifications which is needed in the interim periods before the system described above is to be operating. The hydraulic power supply, using deionized water,

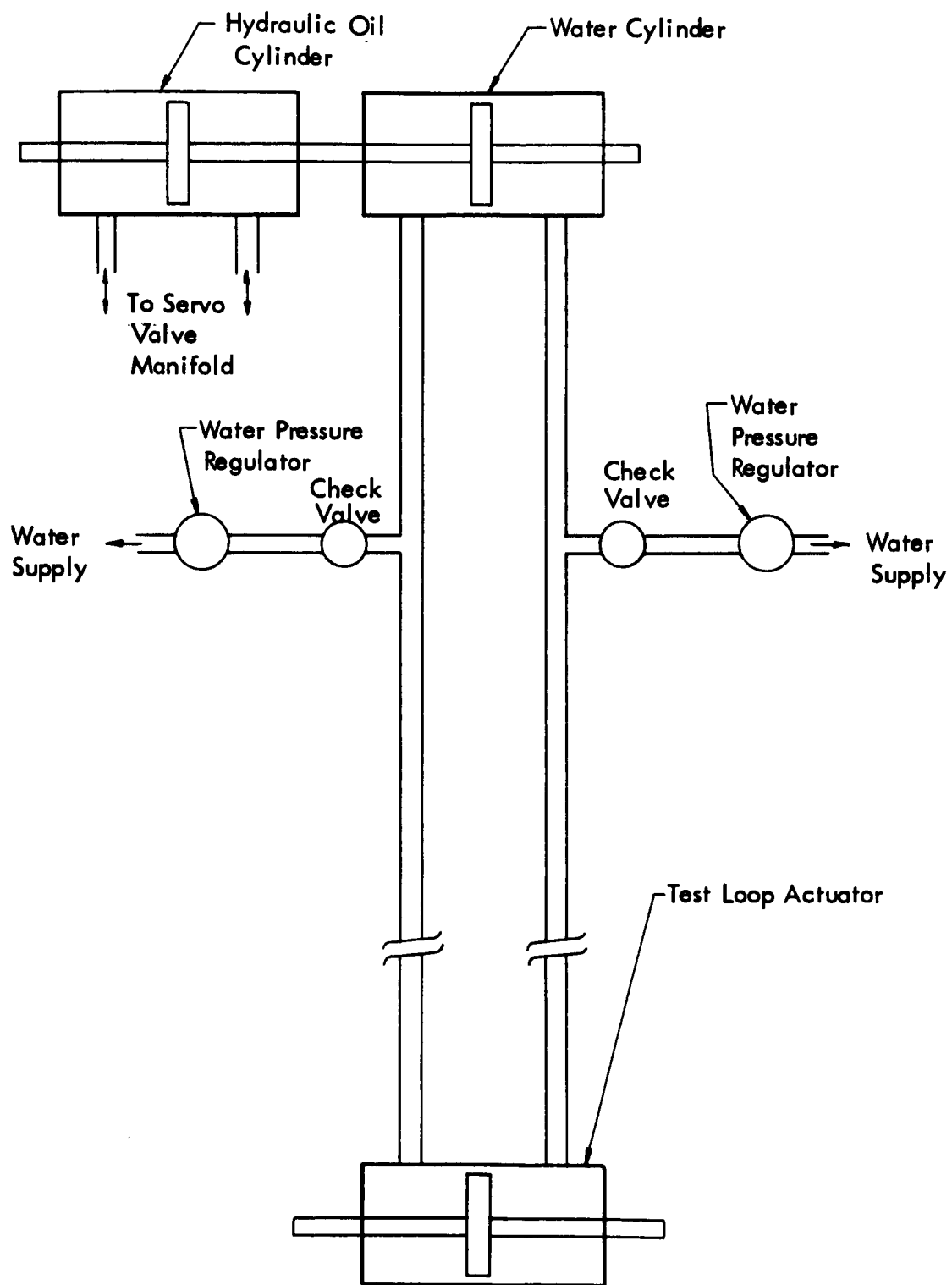


FIGURE 12 OIL PRESSURE TO WATER PRESSURE CONVERSION SYSTEM

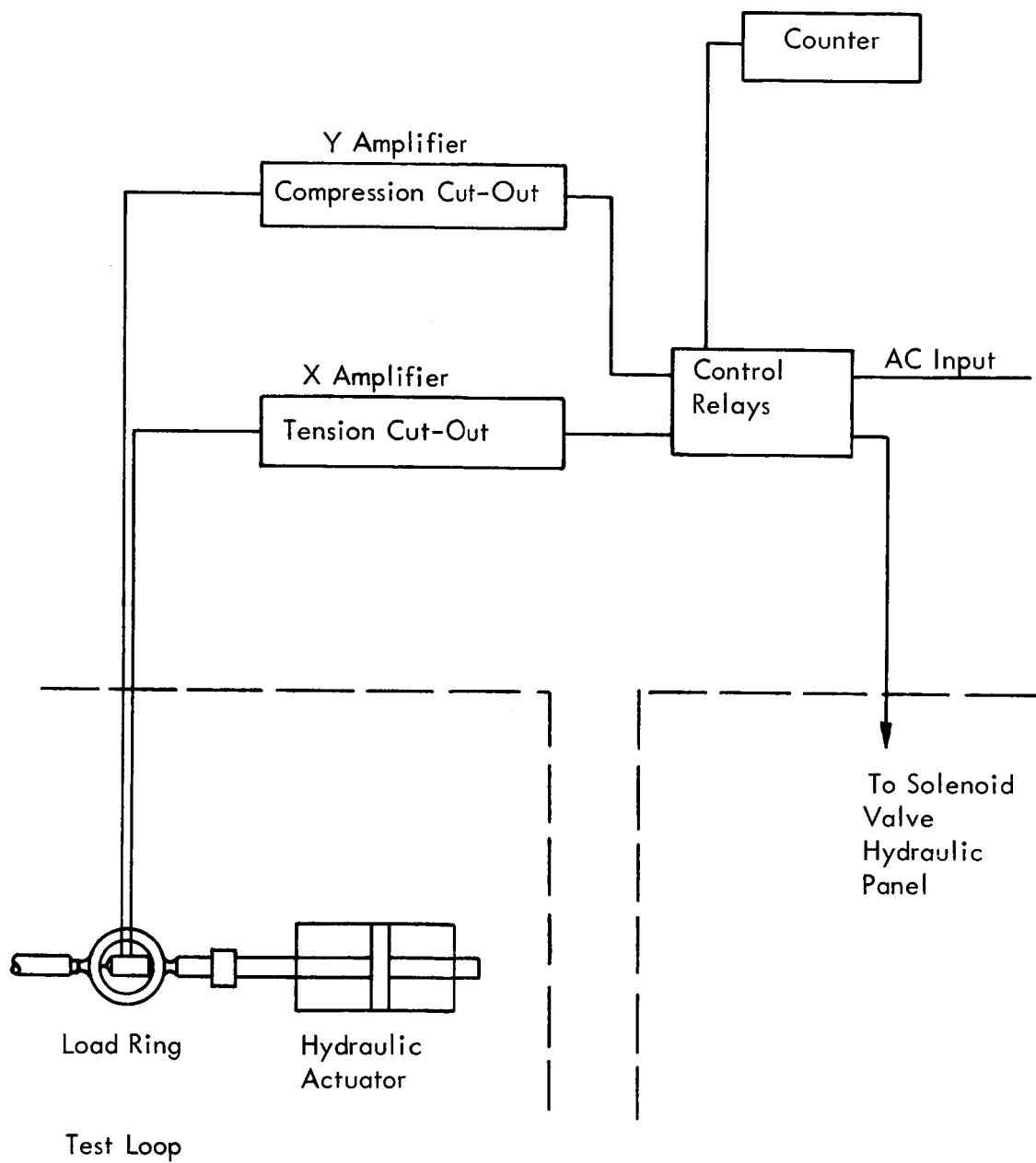


FIGURE 13 ELECTRICAL CYCLE CONTROL SCHEMATIC
PRELIMINARY LOAD CONTROL SYSTEM

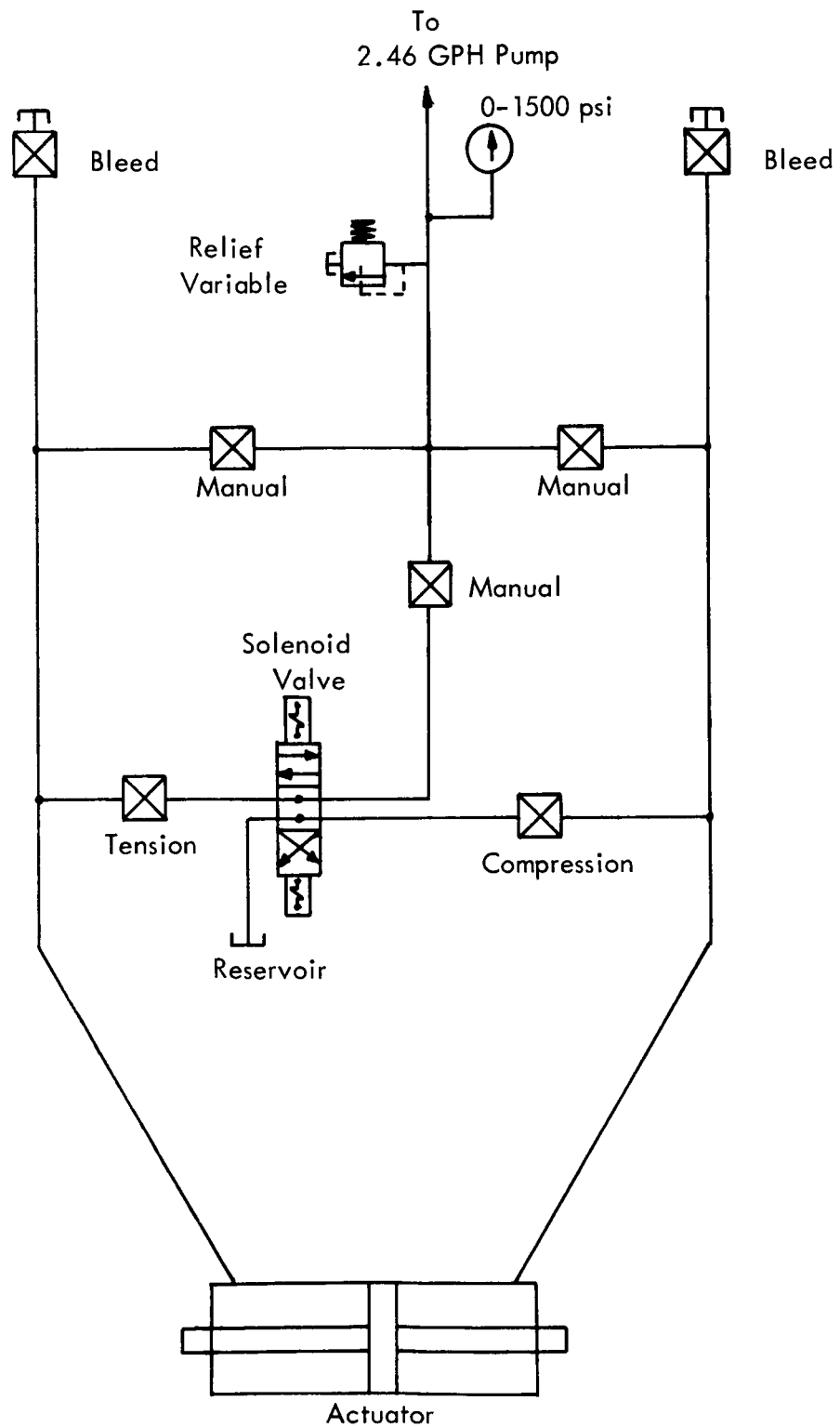


FIGURE 14 HYDRAULIC PANEL CYCLE CONTROL SCHEMATIC
PRELIMINARY LOAD CONTROL SYSTEM

for this system has been the 2.5 gph diaphragm type pump normally used to supply the water to pressurize the beam port seals.

Since this pump will be needed for the tensile testing phase of the contract, another diaphragm type pump has been ordered and will be utilized for additional preliminary development work as soon as it arrives. It will be integrated into the preliminary control system for use as required until the final control system arrives at which time it will serve as a spare unit for the seal water pressurizing system.

3.5 TRANSFER SYSTEM

To permit insertion and withdrawal of the test loops at the beam port and the hot cave, a special transfer system is installed in Quadrant "D" of the Plum Brook Reactor Facility. The location of this system with respect to the reactor beam port HB-2 and the specimen change hot cave is shown in Figure 1. All of the transfer equipment is hydraulically powered (demineralized water as the working fluid) and operates under some 20 feet of quadrant water.

This transfer system will be used throughout the test program both for tensile testing and for fatigue testing.

3.5.1 Design

A schematic of the transfer system is shown in Figure 15. The system includes two base tables, fastened to the floor of Quadrant "D", on which are located translating tables capable of movement in the east-west direction. On each of the translating tables there are three sets of tracks on which specially designed carriages travel to transfer the test loops to the desired location. The lateral east-west translation of the transfer tables allows the positioning of any track in proper alignment with the beam port or the hot cave port for insertion of the test loop. The north table, associated with the hot cave, has the additional capability of rotation through 180° to enable insertion of the forward end of the test loop into the hot cave. The actuating force for this translation and rotation is provided by a 10HP hydraulic pump, using demineralized water as the working fluid. Mechanical stops are situated at the limits of table travel and movable mechanical stops are so located to insure accurate positioning of the tracks for beam port and hot cave insertion of the test loops.

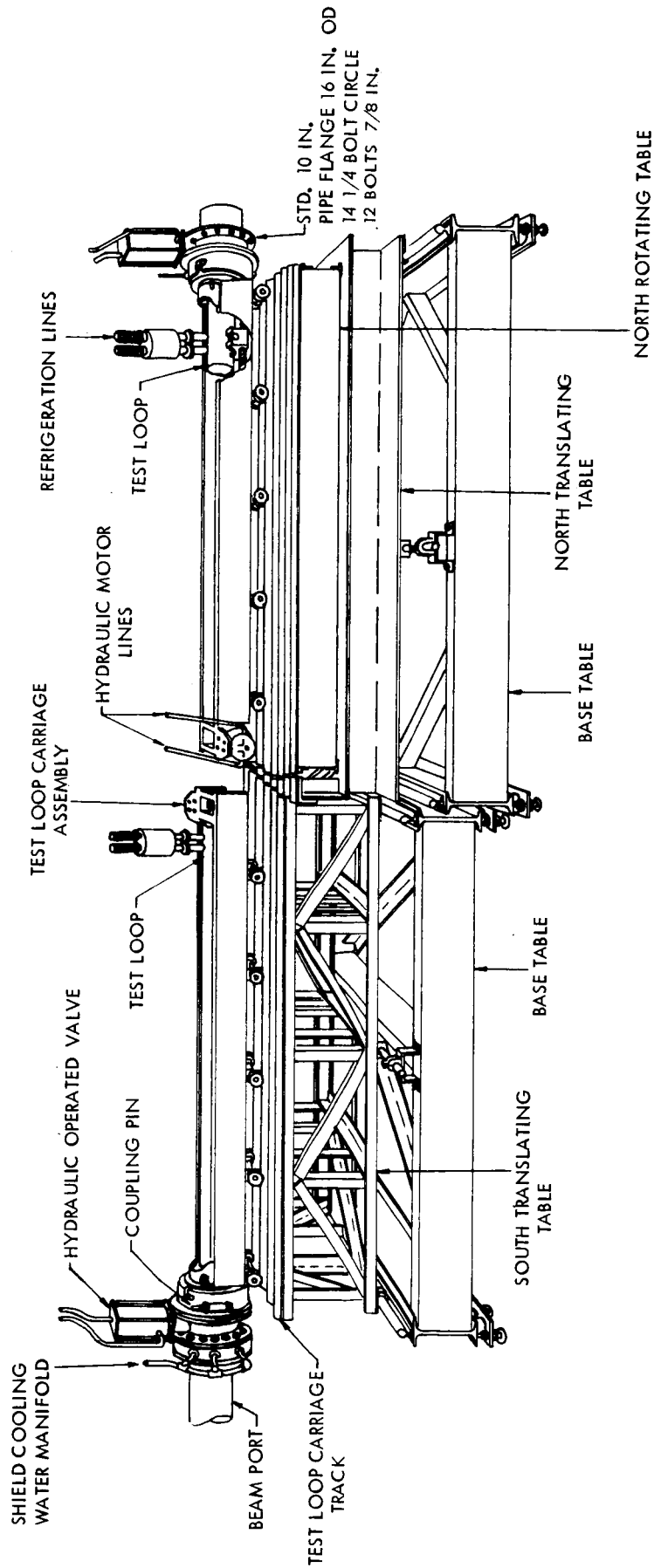


FIGURE 15 TEST LOOP TRANSFER SYSTEM

Each of the carriages which hold the test loops travels on grooved wheels on the table tracks. They are moved on the tables by a hydraulically operated rack and pinion gear actuated by a hydraulic cylinder which is driven by the 10HP pump. By suitable manipulation, the carriage may be placed on any track of the tables and positioned in front of either the beam port or the hot cave. Limit switches located on the tables are tripped by actuators on the carriages and indicate carriage locations on the tables by means of lights on the control console. Mechanical stops limit carriage travel on the tables.

After a carriage is positioned in front of the beam port or hot cave, it is advanced and coupled to the port. Both the beam port and the hot cave port are protected by 6 inch gate type valves. On the quadrant side of each valve there is a chevron seal to prevent water flow past the loop during operation. The valves are interlocked with limit switches to prevent opening unless the test loop is in position in the chevron seal to block flow. After coupling the carriage to either valve, the loop is advanced into the beam port or hot cave by a high torque hydraulic motor driven by the 10HP pump. The torque is translated from the motor shaft to a lead screw through a worm-worm gear connection. This lead screw is coupled to a yoke assembly on the carriage which supports the aft end of the test loop. As the lead screw advances the test loop, limit switches on the carriage indicate the loop position by lights on the control panel. A mechanical stop precludes the possibility of inserting the loop into HB-2 to a point which will restrict the coolant passage between the forward end of the loop and the gamma shield. The test loop drive system, during an insertion into the beam port, must overcome both the primary coolant pressure of 125 psi and systematic frictions. This requires a thrust force of over 4000 lbs.

Limit switches and mechanical stops have been installed at all places necessary to insure safe operation of the transfer system.

3.5.2 Modification

After installation of a new beam port shield in the HB-2 beam port, internal measurements of the shield indicated that the carriage assemblies manual stop as well as the limit switch which determines the "full-forward" position of the test loop in the beam port had to be re-located to allow 0.25 inch additional test loop insertion which is permitted by the internal dimensions of the new shield. This has been done and re-alignment of the transfer system has been completed. Further modification of the transfer system during the test program is not anticipated.

3.5.3 Performance

Pre-neutron procedures were performed using test loop 201-003. These procedures were witnessed and approved by NASA Plum Brook Reactor Facility personnel.

With installation of the new beam port shield, the throttling arrangement of the shield cooling water was changed in such a way as to increase the water pressure within the shield from 125 psi to about 150 psi. This change increases the force on the end of the test loops and thus requires additional thrust to drive the test loop into the beam port.

There is a limitation of 550 psi, imposed by the NASA Plum Brook Reactor Facility, on the carriage drive motor hydraulic pressure which, with the increased back force on the test loop, is just sufficient to drive the loops into the beam port when the carriages are in top operating condition. An increase in the limitation to 750 psi, which is well below the design pressure of 1000 psi, would be sufficient to drive the loops without excess down-time to maintain the carriages in top condition.

3.6 SAMPLE CHANGE EQUIPMENT

Due to the high activity level of the test loops after several in-pile exposures, remote handling techniques are required for changing specimens or routine loop maintenance. To provide operator shielding during work on the test loops, a hot cave was installed outside the wall of Quadrant "D" with the access port on a radial line with HB-2.

3.6.1 Design

The hot cave (Figure 16) is located on the minus 25-foot level directly in front of the external center pool port in quadrant "D". This port is straight across the pool from the HB-2 beam port, which is used in the test program. The walls of the cave, with the exception of the front, are of high density concrete, thus minimizing space requirements consistent with minimum cost, and reducing interference with experiments that might be conducted in adjacent beam ports. Since the working space between the front wall of the cave and the containment vessel is limited, the front wall is a steel structural assembly filled with lead shot. The hot cave structure supports and houses the miniature Model 8 manipulators and the lead glass viewing window. Interior illumination is provided by high intensity mercury vapor lamps

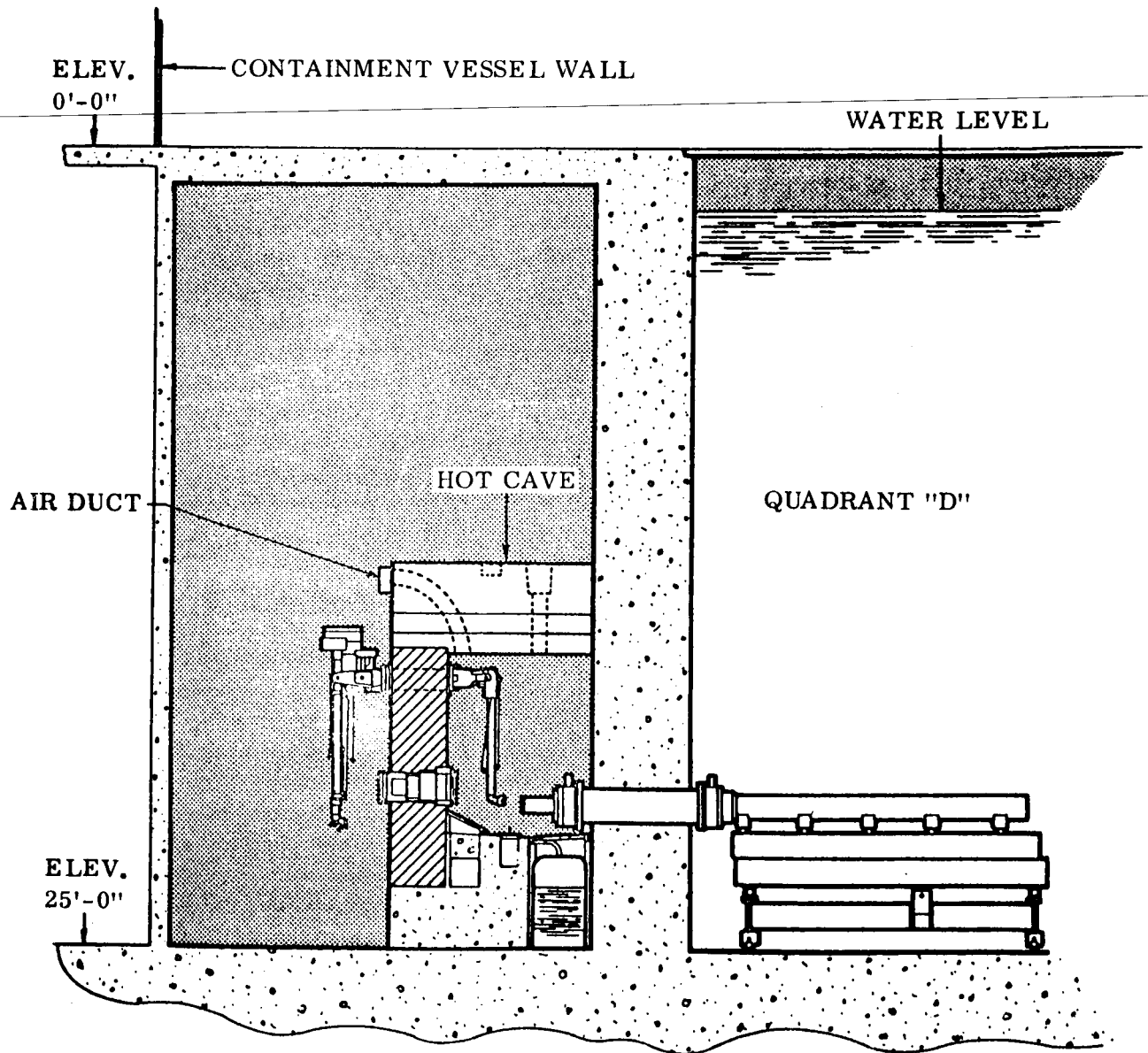


FIGURE 16 HOT CAVE

located within the hot cave. (The quantity of mercury that is in the lamps is less than 80 milligrams.)

A drain system removes any water that may leak from the pool during transition of the test loop through the entrance port, and warm waste materials generated during decontamination activities. This waste material is held in a hold tank located within the cell until such time as it may be pumped into the building drain system. To further aid in decontamination, the interior of the hot cave is coated with a chemically resistant, phenolic base, paint which is, in turn, covered with a polyvinyl strip coat. The ventilation system is self-contained and is not connected to the building system. The air is filtered through an inlet filter, a roughing filter, and an absolute filter to eliminate any radioactive contamination, and is vented to an exhaust stack. When the ceiling block is in position, the ventilation system maintains a normal air flow of 80 cfm through the hot cave. When the ceiling block is removed, the air velocity through the opening is 75 ft. per minute. When the ceiling block is in its nested position a negative pressure differential is maintained inside the cell.

Following installation and during the initial performance of a screening test program, the external surfaces of the hot cave were monitored by the Health Safety Office during each insertion of an irradiated test loop. Since the principal gamma source in an irradiated test loop is Mn^{56} , this practice was discontinued after the loops received sufficient in-pile exposure to saturate the contained manganese.

The hot cave effluent gases are monitored at intervals for possible radioactive release through a particulate filter. In no instance during normal hot cave operation has a significant discharge been detectable.

3.6.2 Modification

No modifications to the hot cave are anticipated during the performance of this test program.

3.6.3 Performance

No serious difficulties have been encountered in operating the hot cave.

3.7 MISCELLANEOUS TEST EQUIPMENT

Although the hot cave has been used successfully for minor repairs in the forward section of test loops, major overhaul and maintenance work on the aft portion of the test loop cannot be accomplished in this area. To provide a capability for removal of the test loops from the containment vessel to the hot laboratory area, a lead filled stainless steel cask (Figure 17) is available. This steel cask was built to provide adequate shielding of irradiated test loops during transfer to the hot laboratory area or during storage outside of the quadrant. The thickness of lead at the activated end of the test loop is 8 inches. The shielding integrity of the cask was demonstrated by moving an eleven curie cobalt-60 source longitudinally through the central axis of the cask while monitoring the exterior surfaces. A manually operated clam-shell lifting device inside the containment vessel permits the insertion of an irradiated test loop into the cask using quadrant water as a biological shield during loop manipulation. A similar, but remotely operated, lifting device is available to facilitate loop handling in the hot laboratory area. After placement in the lead filled cask, the irradiated loop can be removed from the containment vessel through an airlock penetration of the vessel wall without compromising vessel containment. A special bridge over Canal "E", inside the containment vessel, and a special cart outside the vessel facilitate transfer of the cask through the airlock penetration.

During this reporting period, numerous test loop transfers between the reactor quadrant and the hot handling area have been made. The cask has been used for this purpose as well as providing shielding in the hot handling area during certain phases of test loop inspection and repair.

3.8 TEST EQUIPMENT MAINTENANCE AND CALIBRATION

During this reporting period a maintenance and calibration program was instituted in coordination with the requirements of the Plum Brook Reactor Facility. Also, during this reporting period a number of unanticipated difficulties arose due mainly to helium leakage in the test loops.

3.8.1 Maintenance and Calibration Schedule

A maintenance schedule was established for the refrigerator system, the test loops and transfer equipment during a recent major maintenance program.⁽²⁾ These

(2). Summary Report, NASA CR-54770.

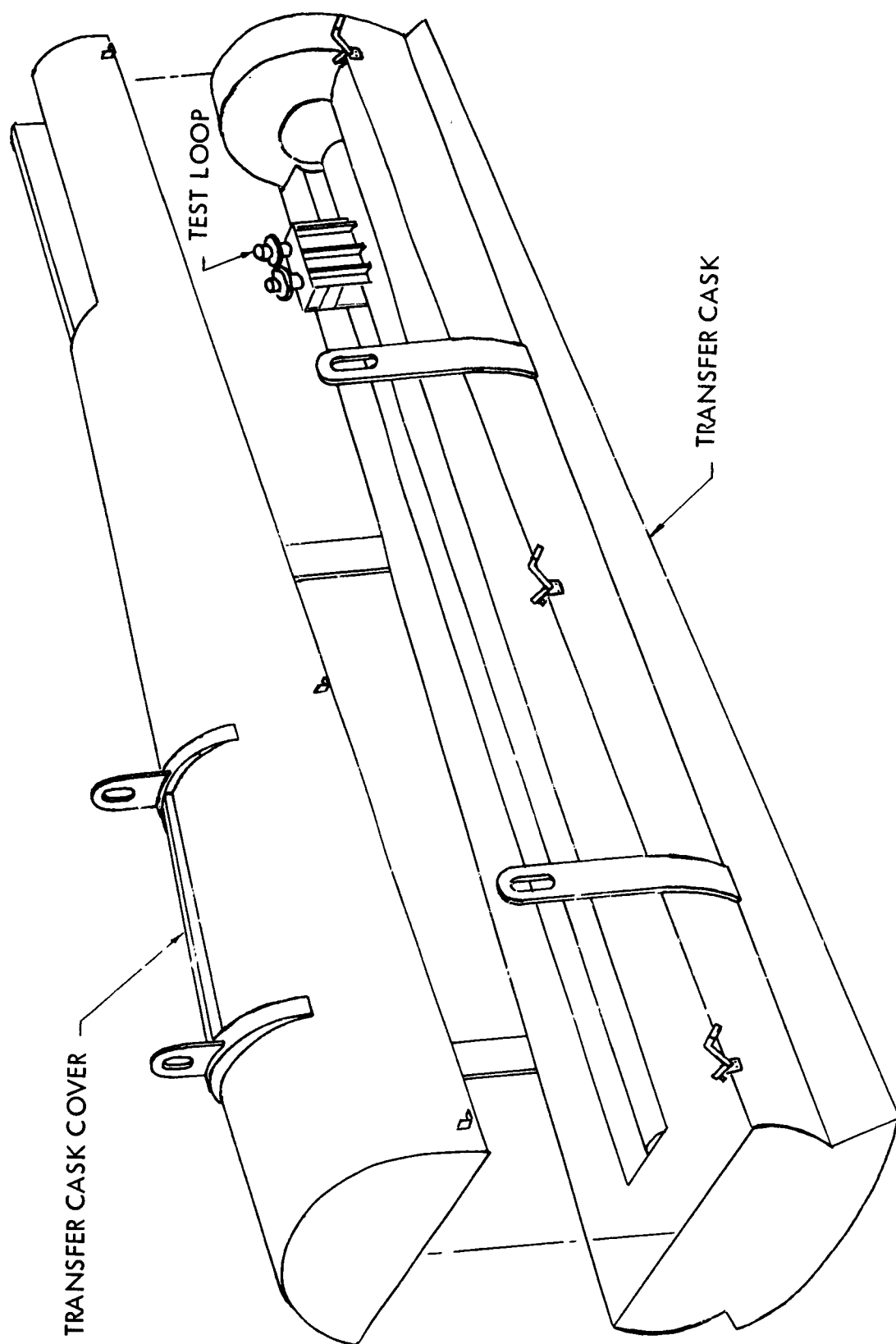


FIGURE 17 CASK

schedules were predicated upon recorded operational history of the system prior to the initiation of the maintenance effort. Where recorded operational time histories had been maintained these were used to determine mean time between failure and a limited reliability evaluation was performed. The results were used to develop periodic maintenance schedules by relating reasonable reliability values to the equipment operation during a typical irradiation test cycle.

A cycle is defined as follows:

- . Insertion into hot cave for specimen installation.
- . Removal from hot cave after specimen installation.
- . Insertion into beam port for test irradiation.
- . Withdrawal from beam port after completing test, and positioning the loop for insertion into the hot cave for specimen change-over.

The operation of various equipment versus time in such a cycle is shown in Figure 18, and the periodic expansion engine maintenance schedule, so developed, is shown in Figure 19.

Six expansion engines are available for use in the refrigerator system. The normal application requires four of these engines to be installed in the system and two are maintained as spares. The total accrued time on these engines since installation of the refrigerator system at the reactor site is as follows:

	<u>September 20, 1965</u>	
Engine No. 1	5417.7	hrs.
Engine No. 2	5329.5	hrs.
Engine No. 3	4163.0	hrs.
Engine No. 4	3532.4	hrs.
Engine No. 5	4389.5	hrs.
Engine No. 6	3296.1	hrs.

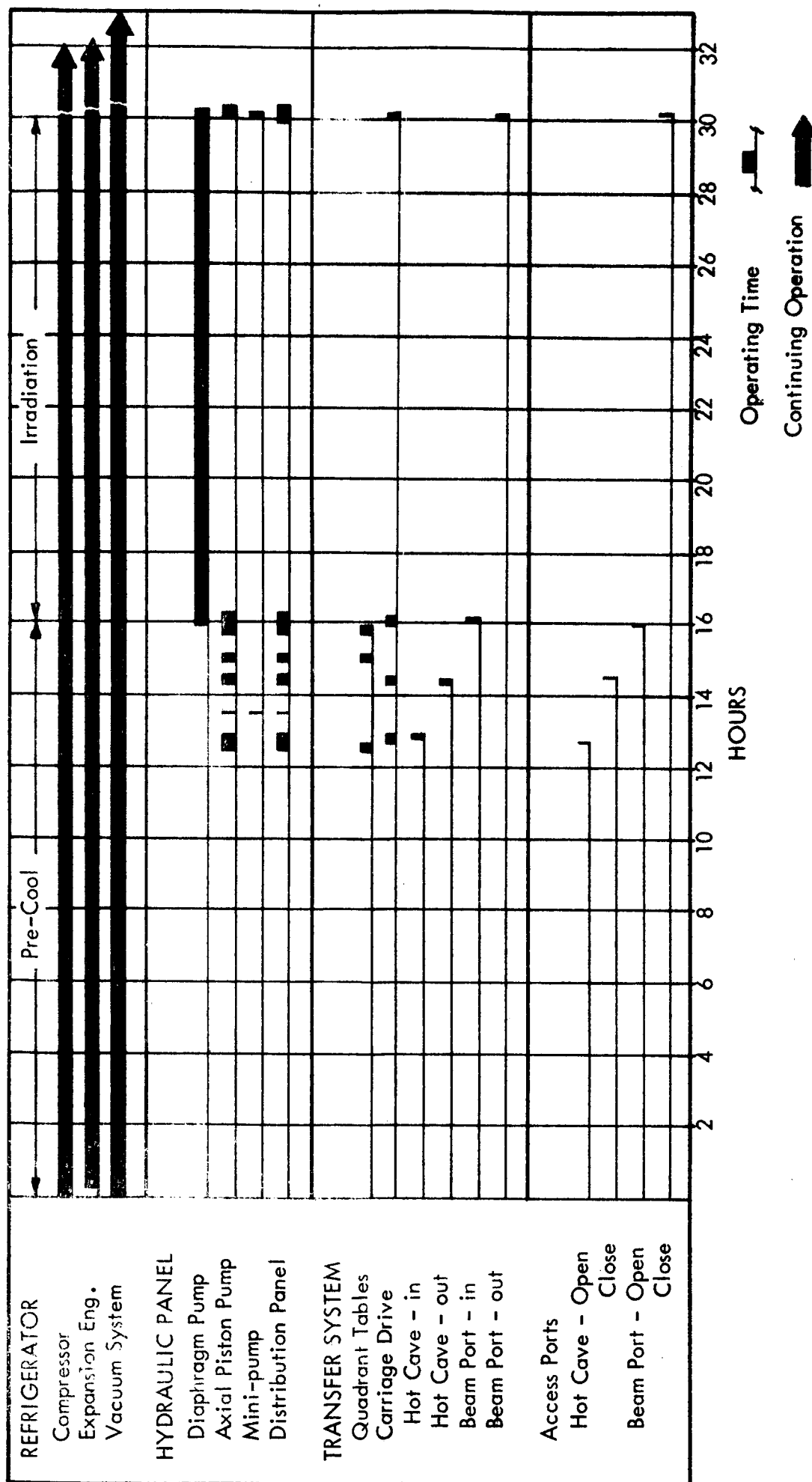


FIGURE 18 EQUIPMENT OPERATION TYPICAL IRRADIATION TEST CYCLE VS. HRS.

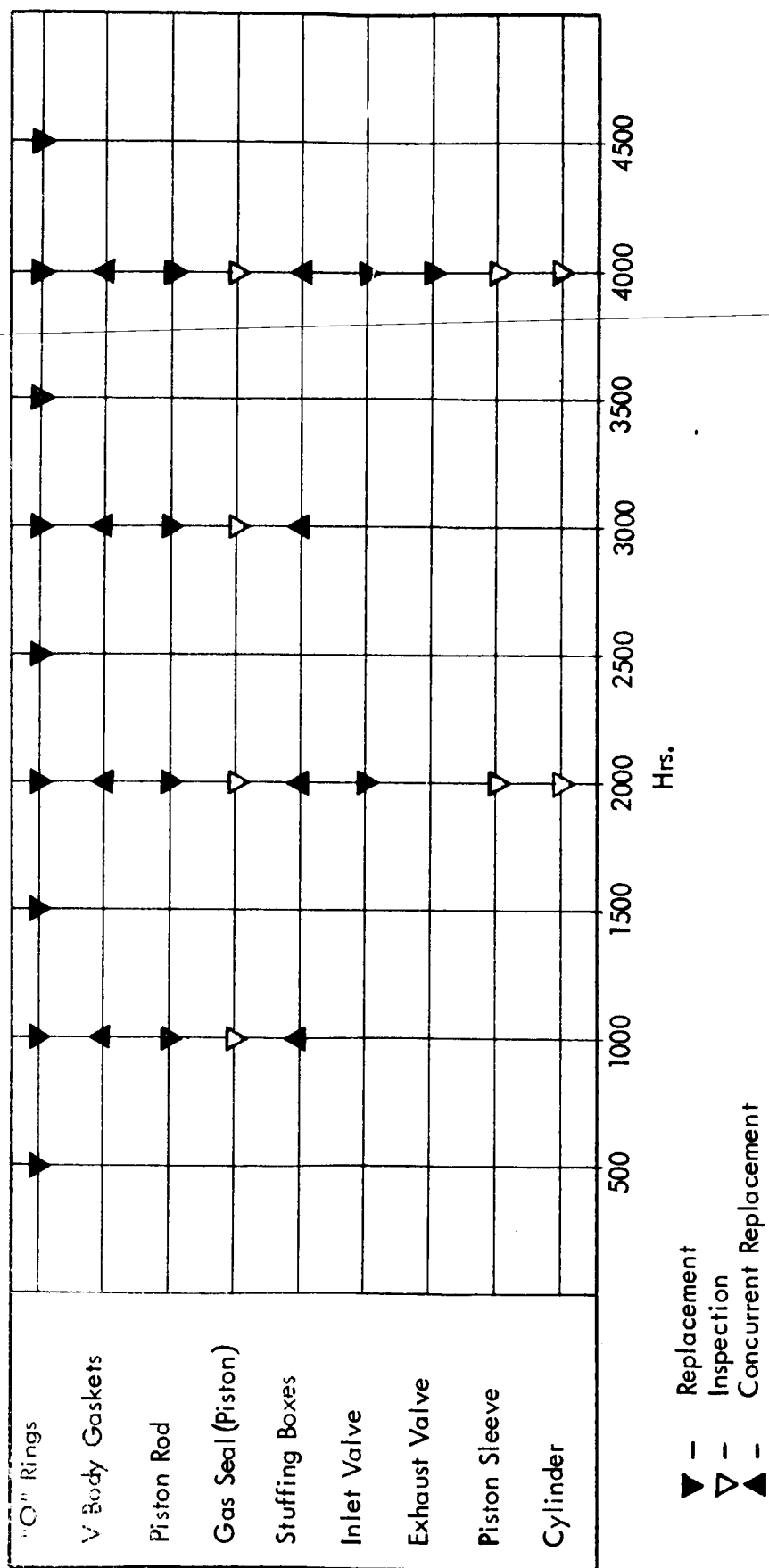


FIGURE 19 EXPANSION ENGINE MAINTENANCE SCHEDULE

The system was recently overhauled and the engines were used to provide refrigeration to various parts of the system for low temperature evaluation and to perform calorimetric tests on the refrigerator system to provide refrigeration capacity at various temperature levels. More recently the system has been used to establish operating criteria for the forthcoming test program.

No. 1 and No. 2 pods have been operated for 63.7 hrs. and 85.4 hrs. respectively. The engines in pod No. 2 have been changed once. The reason for the change was the collection of moisture in the engine and on the valve faces causing degradation of refrigerator capacity.

The other equipment in the test system does not have recorded operating time histories but the records indicating the number of times the equipment has been used in tests were maintained. As a result the schedule in Figure 20 was developed using cycles of operation as the parameter.

Limitations in rigorously applying schedules are defined and include such items as correlating quadrant maintenance with draining schedules and refrigerator maintenance with down periods of the reactor. The schedules shall be applied so as not to interfere with normal reactor or test operations.

Maintenance logs, containing forms, compatible with these maintenance requirements have been devised to provide an easily accessible indication of forthcoming maintenance requirements.

3.8.2 Repairs And Adjustments

3.8.2.1 Tensile Test Loops

The temperature correlation program for tensile tests was initially intended to be performed in test loop 201-004 but excessive heat load at 30°R indicated a leak in the test loop. The test loop was removed to a position over the hot dry storage area in the Hot Materials Laboratory for repair. Subsequent investigation indicated a leak in the front face of the evacuated chamber at the forward bulkhead. Another leak was detected in the front bearing housing which supports the forward end of the actuating rod. Both of these leaks were repaired but the thermocouple extension leads were damaged in the process. A thermal shock and subsequent soaking of the helium chamber in the test loop in LN₂ indicated that the leaks into the evacuated annular space were eliminated. Minute leakage was indicated, however, in the

- ▽ Inspection & Adjustment if Required
- ▽ Disassembly and Inspection
- ▼ Replacement Overhaul
- f Fatigue Equipment

50

bellows assembly (see Figure 6) which provides a seal between the helium and the cooling water while still allowing the actuating rod to traverse. This leakage was repaired by the use of soft solder over the affected area. Another thermal shock with LN₂ and subsequent actuating of the bellows for 20 cycles produced no leaks discernible by the helium leak detector. The thermocouple leads were replaced in the loop and the out-of-pile temperature correlations were performed with this loop.

Test loop 201-002 was prepared for the temperature correlation tests as soon as difficulties were encountered in test loop 201-004. A temperature correlation with the platinum resistance thermometer package was performed with the loop but it was noticed that a leak into the evacuated annular space developed at 30°R as indicated by a rise in pressure on the thermocouple gage used to monitor the vacuum in the helium transfer lines in the test loop. This leak closed as the refrigerator temperature was raised to about 70°R. Several cycles verified this phenomena. No further testing was performed as the loop was removed to the Hot Materials Laboratory for further investigations. Leakage in the front section of the evacuated chamber in the forward end of the bulkhead was detected and repaired. Leakage in the bellows similar to that found in test loop 201-004 was also repaired and the test loop appeared to be leak free. A LN₂ thermal shock and soaking for more than 2 hours has now shown that leakage exists in one of the helium transfer lines. The leak apparently is located at the aft weld joint between the bellows and the inner helium transfer line. Methods of repairing this leak are still being investigated.

The discovery of leaks in the actuating rod bellows assembly on test loop 201-002 and 201-004 prompted a check on test loop 201-003. It was thermally shocked and soaked in LN₂ and a subsequent check with the helium leak detector disclosed a leak in this bellows also. Since the leak detector indicated that all of the leaks in the bellows were minute, the bellows was immersed in water and internally pressurized with helium at 35 psi to ascertain if visual leakage in the form of bubbles could be determined. There was no leakage evident. It was therefore decided that the leakage was so minute that no difficulties would be encountered in the use of this loop for in-pile testing.

Since test loop 201-002 has not been repaired to date, test loop 201-003 will be used for the initial flux measurements in HB-2 as well as the ensuing test program.

3.8.2.2 Test Loop Head Assemblies

In the interest of getting all equipment ready for resumption of an in-pile test program,

irradiated test loop head assembly 201-007 was made ready for re-evacuation without incorporating the blank-off cup in the nuclear instrumentation tube. During the leak check at a temperature of 375°F, however, a leak in the bellows was discovered making further evacuation unfeasible. Since head 201-008 was already known to have a leak in the bellows assembly and a blank-off cup has not been successfully welded into head 201-010, the three irradiated head assemblies cannot be used unless a method of repair is found.

A study is presently underway to try to repair head 201-010 while another study to determine the cause of failure in the bellows assembly is also being carried on. A cask shown in Figure 21 is being fabricated to transport test loop head assembly 201-010 to Lockheed-Georgia Nuclear Laboratories for repair of the hole in the nuclear instrumentation tube.

3.8.3 Corrosion of Test Equipment

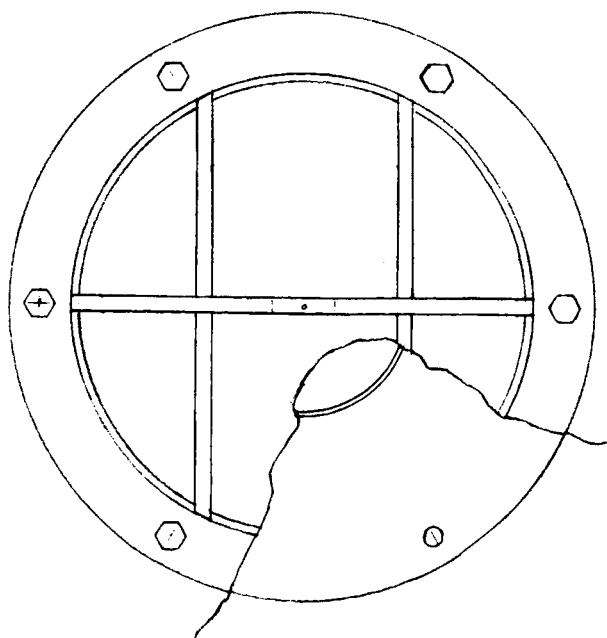
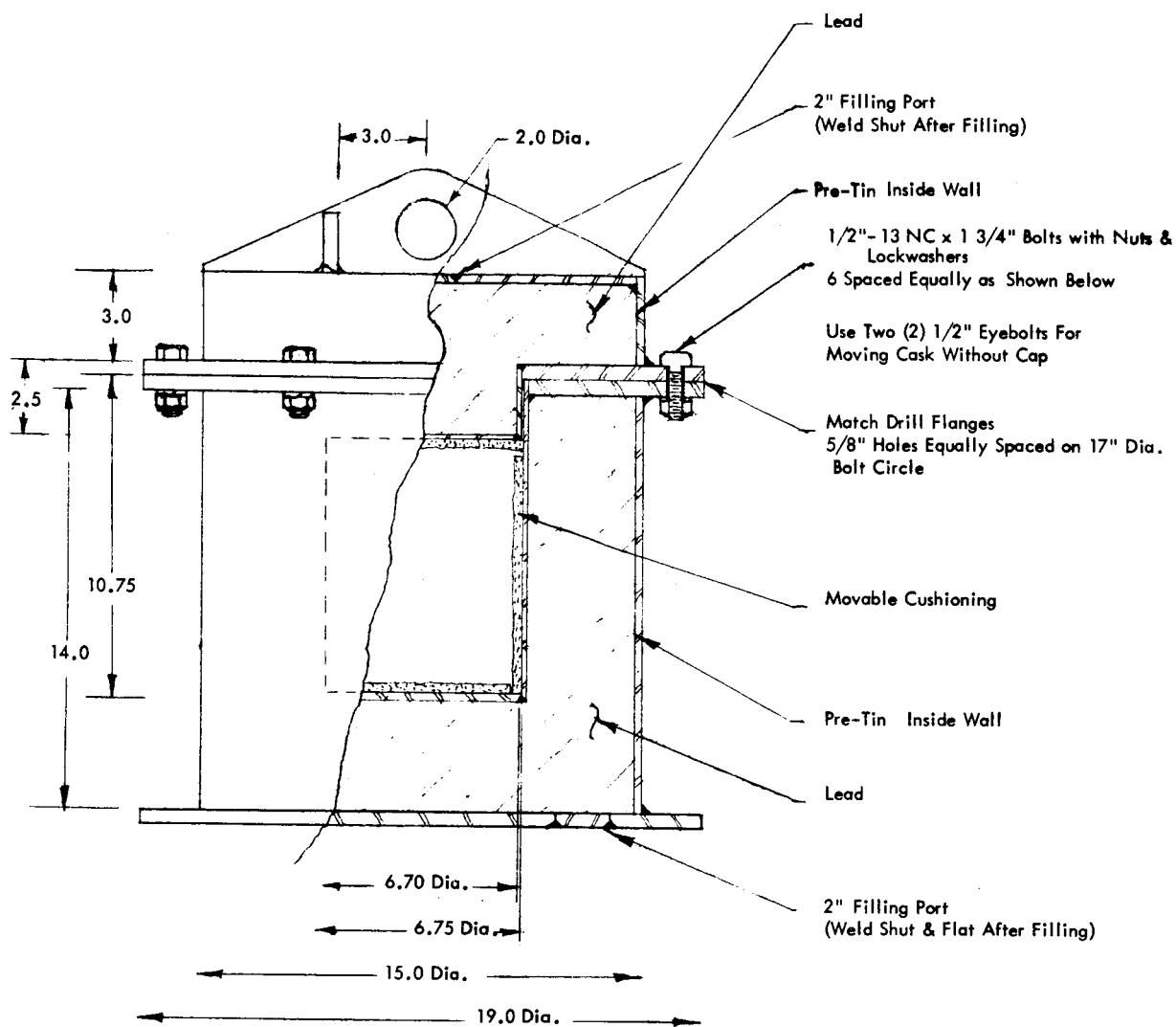
A number of problems which have come to light during this reporting period can be attributed to corrosion.

The aforementioned leakage in the actuating rod extension bellows is accessible and appeared at or near the peripheral weld in the bellows assemblies. Such leakage, although minute now, is serious in that if it should become more extensive, it would allow leakage of helium into the quadrant water or primary water into the helium gas when the test loop is inserted into the beam port.

Also, the bellows in the head assembly, which reduces thermal stress due to differential thermal expansion in the head, have shown leaks. Although these could not be located exactly and the cause of these leaks has not been established, the bellows are of the same construction as the actuating rod bellows and so may be subject to similar failure.

The dynamometer load rings, which are machined from a nickel bearing steel and nickel plated, show a pitting type of corrosion which was not sufficient to affect the load ring characteristics but which is important because of the apparent corrosion problems which have appeared more recently. The corrosion products from the load ring may accelerate corrosion elsewhere in the loop.

Because of the seriousness of the problems, and because first inspection indicated that the leaks in the extension bellows probably resulted from corrosion, a corrosion



MATERIALS:
Cask Filled As Shown With Lead

304L
SST

1/2" Flanges & Bottom Plate,
Hanger & Gussets
1/4" Outer Shells, Top Plate
& Inside Bottom Plate
1/8" Inner Shells & Inside
Top Plate

1/2"-13 NC x 1 3/4" Bolts
With Lock Washers & Nuts

FIGURE 21 TEST LOOP HEAD ASSEMBLY CASK

engineer with broad experience in this speciality, was called in from the Lockheed-Georgia Company for an opinion on the cause. The conclusions of what could be done to correct the problem temporarily without replacement of the bellows which would cause a long delay in the use of the loops, and what could be done to prevent re-occurrence of this trouble are as follows:

- 1) The intermittent immersion in deionized water to which the bellows are subjected is a very severe corrosive condition which no stainless steel, particularly thin gage and welded, can be expected to withstand for long periods of time. The passivating oxide layer which stainless steels require for corrosion protection may break down even without galvanic action and corrosion may be intensified by the presence of corrosion products from other sources, such as the dynamometer proving ring.
- 2) The leaks in the bellows assemblies should be expected to become more extensive with time since the environment cannot be changed.
- 3) Soft solder of the bellows with special care to not leave a flux residue, which would contain chloride ions that induce stress corrosion, would be a satisfactory temporary measure for eliminating leaks as they appear.
- 4) The bellows assemblies should be replaced as soon as possible by one of different design with less welding.
- 5) Crevices should be avoided wherever possible.
- 6) The new bellows should be carefully heat treated (depending on the steel used) following welding to reduce stress corrosion and then pickled if necessary and carefully passivated before installation.
- 7) The installation welds should be pickled and passivated in place.
- 8) The whole assembly should be passivated at intervals during operation depending on the appearance of any corrosion products because of the severe environment.

- 9) The load ring should be replaced by one of a different alloy or by one of the same alloy with a fatigue and corrosion resistant nickel plating. (.003" if possible, by the Barrett process.)
- 10) The head assembly bellows, although not subjected to water, may be exhibiting the same type of corrosion with the additional factor that stresses and consequently stress corrosion would be more pronounced in this bellows.

3.9 EXPERIMENT DESIGN MANUAL AND HAZARDS ANALYSIS

The Experiment Design Manual and Hazards Analysis have been updated at intervals throughout operation of the test equipment with the most recent change being to include a hazard analysis for operating the test loops at temperatures above 30°R. This analysis is complete and includes activation analysis of each impurity gas that may be exposed to irradiation and eventually released to the atmosphere at various operating conditions and with the consideration of possible sudden releases of the contained gases from various points in the system.

Changes in the Experiment Design Manual will be required to cover the modification of the test equipment for the fatigue testing but no additional hazards analysis is anticipated.

4 TEST PROCEDURES

Certain procedures, preliminary to actual testing of specimens under the required controlled environment, are necessary as the result of a new beam port shield and the broad scope of the test program. Calibrations in the form of neutron flux mapping and temperature correlations and a new fatigue specimen design are required. As in the screening program, standard tensile test specimens cannot be used in this test program due to various restrictions on the test equipment imposed by the nuclear cryogenic environment. Although fatigue specimen design is not as standardized as tensile specimen design, the fatigue specimens used in this program will represent a departure from any commonly used design.

4.1 TEST SPECIMEN DESIGN AND FABRICATION

4.1.1 Tensile Specimens

The tensile specimens to be used in this program represent a miniaturization of the standard ASTM E-8 Specimen.⁽³⁾

The nominal diameter of the mid-point in the gage length is 1/8 inch. The gage length is nominally 1/2 inch to maintain the standard 4:1 gage length to diameter ratio.

The limits of the gage length are delineated by light sandblasting of gage marks over an area 1/16 in. x 1/8 in. at each end of the gage length. This method of marking was used to avoid introducing a notch at each end of the gage length.

The raw material from which the specimens was fabricated was thoroughly inspected using both visual and non-destructive testing techniques to insure uniform material quality of the completed specimens. After final polishing, the finished specimens in each alloy group were checked against each other using Eddy current techniques to assure the homogeneity of each sample lot of test specimens.

During all machining operations unusual precautions were taken to meet the especially strict dimensional tolerances required due to the small size of the test specimens. After machining, each specimen was polished in a longitudinal direction to remove

(3). Anon: ASTM Standards, The American Society For Testing Materials, 1958, Part 3, pp 103-119.

any tool marks or scratches formed during machining. After completion, all significant dimensions were recorded for each specimen using an optical comparator to measure the dimensions.

Sufficient test specimens to complete the current tensile testing requirements of this program have been fabricated and are ready for use.

4.1.2 Fatigue Specimens

A variety of fatigue specimen designs have been considered with the objectives being to: (1) facilitate placement, initial alignment and maintenance of alignment during testing in such a way as to minimize bending moments and any tendency to buckle under compression; (2) minimize slack in the specimen holders; (3) permit cooling of the entire gage length to test temperature by placing adequate surface areas in the helium flow and by reducing volume to minimize gamma heating; and (4) facilitate fabrication without work hardening of the specimen during fabrication.

A preliminary design has been made which will be qualified in a modified test loop with the preliminary load control system described in Section 3.4.2.1 before deciding on a final specimen design and fabricating specimens for the low-cycle fatigue testing requirements of this program.

The preliminary fatigue specimen design represents a compromise between the Wright Field Type⁽⁴⁾ and that used by various experimentalists including L.F. Coffin, Jr.,⁽⁵⁾ reporting results of low cycle fatigue testing in the open literature. It is essentially a large radius notched bar with threaded ends for rigid gripping. The minimum diameter is 0.125", the surface radius is 0.75", the threads are 3/8"-24 NF-2, the over-all specimen length is 2.125". The "gage" length is approximately 0.8".

This specimen will be relatively easy to mount into and remove from the test loop remotely and will give adequate resistance to buckling under compression with reasonable stress and temperature distributions. With this specimen design the new specimen holders will be nearly identical with those used in the screening program with the major change being the addition of jam nuts to secure the specimen in the holders with minimum slack in the threads. A new bushing in the head assembly will be required to distribute the tension and compression loads while maintaining

(4). Anon., Manual on Fatigue Testing, ASTM Special Technical Publication No. 91, 1949, p 32.

(5). L.F. Coffin, Jr. and J.F. Tavernelli, The Cycle Straining and Fatigue of Metals, Trans. AIME, Vol. 215, Oct. 1959, p 794.

alignment. Anticipated possible changes after preliminary testing will be the addition of stress relief notches at the ends of the "gage" length and in the threads at the jam nut and holder juncture and possibly the addition of extended heat exchanger surfaces to the holders.

A specimen placement procedure has been prepared on the assumption that the final specimen and specimen holder designs will not differ much from the preliminary design. It does not appear that additional special tools or jigs will be required.

Some stress analysis and heat transfer analyses were undertaken during this reporting period and the resulting qualitative conclusions should be useful to the analysis of the test results or to more refined heat transfer studies that may prove necessary in the event that severe alignment or gamma heating problems are encountered during the preliminary testing.

Although not ordinarily considered in the presentation of fatigue data from similar specimens, there are stress concentration (or fatigue notch) factors in this type specimen due to the variation of cross section of the gage length and due to the threads. Adjustment of the test results due to the notch effect in the "gage" length will be less than three percent.⁽⁶⁾

The maximum elastic strain rate within this specimen is estimated to be an order of magnitude greater than that which would result in a specimen of the same gage length but of uniform cross section under a given specimen total elongation per unit time. With plastic deformation this factor must be multiplied by the ratio of the elastic modulus to the plastic modulus and can be very high in materials such as Aluminum 1099, even at a one cycle per second cyclic rate. This will have to be considered in the evaluation of the test results.

A detailed stress analysis in this specimen, particularly with plastic deformation, is impossible.⁽⁷⁾ Some cursory estimates of maximum tolerable misalignments result in values that are impossible to achieve and this analysis has been abandoned in favor of the experimental approach. The alignment problem with respect to required test loop modifications was discussed earlier in Section 3.1.2.

A number of specimens were machined from 18 Ni 300 Maraging Steel for preliminary testing, including observation of test loop misalignments, as well as to establish acceptable machining and finishing procedures. One of these in the unaged condition has been failed under cyclic loading in the prototype test loop. The load

(6). R.E. Peterson, Stress Concentration Design Factors, John Wiley & Sons, New York, 1953.

(7). L.F. Coffin, Jr., private communication.

was cycled and gradually increased and the specimen failed after 15 cycles with an applied stress of 160,000 psi, which is the approximate ultimate strength of the material in the unaged condition. Inspection of the failed specimen showed no indication of buckling and showed a fracture with necking very much like that for low cycle fatigue failures. This, in itself, is encouraging but more prototype specimen failures under various conditions of aging and loading will be required before definite conclusions can be reached regarding the alignment problem.

Heat transfer studies have been reviewed to determine potential difficulties with respect to temperature distribution in the fatigue specimen and fatigue specimen holder under various gamma fluxes including the maximum gamma flux that might be expected with the new beam port shield (0.40 watts per gram in the head assembly). Anticipated changes in the specimen shape and the specimen holder configuration from those used in the previous test program were also considered.

Analog field plots of the isotherms were made with an electrical analog field plotter to determine effects of various changes in contact resistances and in the heat transfer to the helium. It was assumed on the basis of the older calculations that the worst condition will be in the forward end of the specimen and the forward specimen holder. Conclusions from these studies are as follows.

It will be essential to maintain good heat transfer from the specimen holders to the helium through the jam nuts or other configuration and poor heat transfer from the specimen holder to the specimen (within the limitation that alignment or security of the specimen cannot be sacrificed).

With poor contact with the specimen holder at the end of the specimen, less than 10% of the heat flow to the helium will be through the specimen and the maximum temperature gradient in the specimen is approximately half the maximum temperature gradient in the specimen holder.

Regardless of variations in the contact resistances and heat transfer to the helium, there appears to be a region within the specimen shoulder where the isotherm is always nearly normal to the axis of the specimen. This fact can be used in the event that refined calculations or field plots of the surface temperature distribution prove to be desirable after some temperature distribution measurements in the preliminary fatigue specimen are obtained.

4.2 FLUX MAPPING

Accurate knowledge of the fast flux available in HB-2, both spectral shape and level, is necessary to determine the irradiation exposure required to provide the desired integrated flux for each specimen. This will be accomplished by foil measurements using a combination of low and high threshold energy monitors. Lockheed procured the low threshold energy foils - Neptunium, Uranium, and Sulfur, for this use during this reporting period. The remainder of the foils will be supplied by NASA.

No flux measurements were made during this reporting period. It is anticipated that they will be started in Reactor Cycle 39P, in late October and early November, and reported during the next reporting period.

4.3 TENSILE TEST METHODS

Tensile test methods to be used are the same as those used during the screening program. The only exception results from the necessity of maintaining test loop temperatures above 30°R for certain experiments after changing the temperature in the course of these experiments as indicated by the scope of the testing program to be described in Section 5.

A method for attaining and maintaining the higher test loop temperatures in such a way as to result in a minimum loss of refrigeration time to return the test loop to 30°R will have to be established by experience.

4.3.1 Temperature Correlation and Control

At the outset of the screening program it was planned to monitor the test chamber temperature with a platinum resistance thermometer mounted in the test loop helium inlet duct just aft of the forward bulkhead. However, work reported by Coltman, et.al.,⁽⁸⁾ at ORNL indicated a gross change in the low temperature electrical resistance of platinum resulting from exposure to a fast neutron environment. This irradiation induced increase in resistivity is not completely removed by self-annealing at room temperature. Therefore, location of platinum resistance thermometers

(8). Coltman, R.R.; Klabunde, C.G.; McDonald, D.C. and Redman, J.K.: Reactor Damage in Pure Metals, J. Appl. Phys., Vol. 33, No. 12, December 1962.

as originally planned would require re-calibration after each irradiation. Even after re-calibration, the sensors would have an uncertainty of measurement of about $\pm 10\%$ at the test temperature.

For this reason, two platinum resistance thermometers were installed to monitor the temperature of the inlet and return helium streams in each test loop at a location remote from the fast neutron field. These pairs of sensors were located some thirty feet from the test zone, in the inlet and return legs of the refrigeration manifold.

Since this temperature control method does not provide direct measurement of specimen temperature, relationship between indicated sensor readings and specimen temperature must be determined with thermocouples attached to typical specimens during the following three test stages:

1. Calibration of direct measuring thermocouples on instrumented specimens.
2. Determination of temperature distribution across the gage length of each of the above specimens.
3. Determination of correction to be applied to the control sensors to insure the desired temperature at the gage length mid-point.

The installation of the new beam port shield assembly along with the need for test operational temperatures other than 30°R have necessitated correlation of the test specimen temperature with that recorded by the platinum resistance thermometers located in the refrigerator manifold.

Temperature control at the specimen is maintained by platinum resistance type temperature sensors which are located in the refrigerant distribution manifold. To determine the temperature of the test specimen, recognizing that it is maintained at some temperature between that observed at the manifold sensors, a test procedure which measures the temperature at three points on the specimen was developed.

The specimen selected as a titanium alloy (6Al-4V). This material was selected for the standard since the thermal conductivity of this alloy is typical for alloyed titanium and considerably less than for the commercially pure titanium (55A) or high

purity aluminum (1099). The thermocouple junctions were welded to the bottom of a small axial groove and were located at the midpoint and gage marks on the specimen with the leads also positioned in the groove in thermal contact with the specimen for the maximum available distance. After mounting the thermocouples, the groove was filled with a suitable potting compound to prevent perturbations in the gas flow pattern around the specimen when mounted in the test loop.

The procedure requires the calibration of the copper-constantan thermocouples as attached to the test specimen by using a previously NBS calibrated platinum resistance thermometer as a reference temperature. This thermometer together with the thermocouple instrumented specimen were wrapped with aluminum foil and placed in the test loop so that the helium refrigerant would flow over the package. The leads from the thermocouples were routed aft through available tubes as indicated in Figure 22 and the leads of the platinum resistance thermometers were routed through the end cap as shown in Figure 23.

The temperature of the package was stabilized in the loop by means of the refrigeration system, at approximately 540°R, 320°R, 140°R, 70°R and 30°R.

The EMF generated by the thermocouples relative to an ice bath reference junction were correlated with the temperature measured by the platinum resistance thermometer. The calibration of the thermocouples obtained are plotted in Figure 24. These values were then correlated with NBS tabulated values for copper-constantan thermocouples by overlaying the curve of the calibrated thermocouples on a curve plotted from NBS values. The slope of the curve appeared nearly the same as that for the NBS curve so the $\Delta E \left(\frac{MV}{^{\circ}R} \right)$ values

compatible with the standard were used to determine a correction factor for the thermocouples calibrated in the system. These results are plotted in Figure 25.

Subsequent to this the instrumented specimen was placed in its holder in the normal test position as shown in Figure 26 and test runs at anticipated test temperatures were performed. The refrigerator operation was controlled during these tests to limit the mass flow by reducing engine rpm to a level where the ΔT across the inlet and outlet sensors could be maintained within a nominal operating range; thus, the results reflect conservative temperature differences inasmuch as increasing engine speed increases mass flow reducing all temperature differentials in the test system.

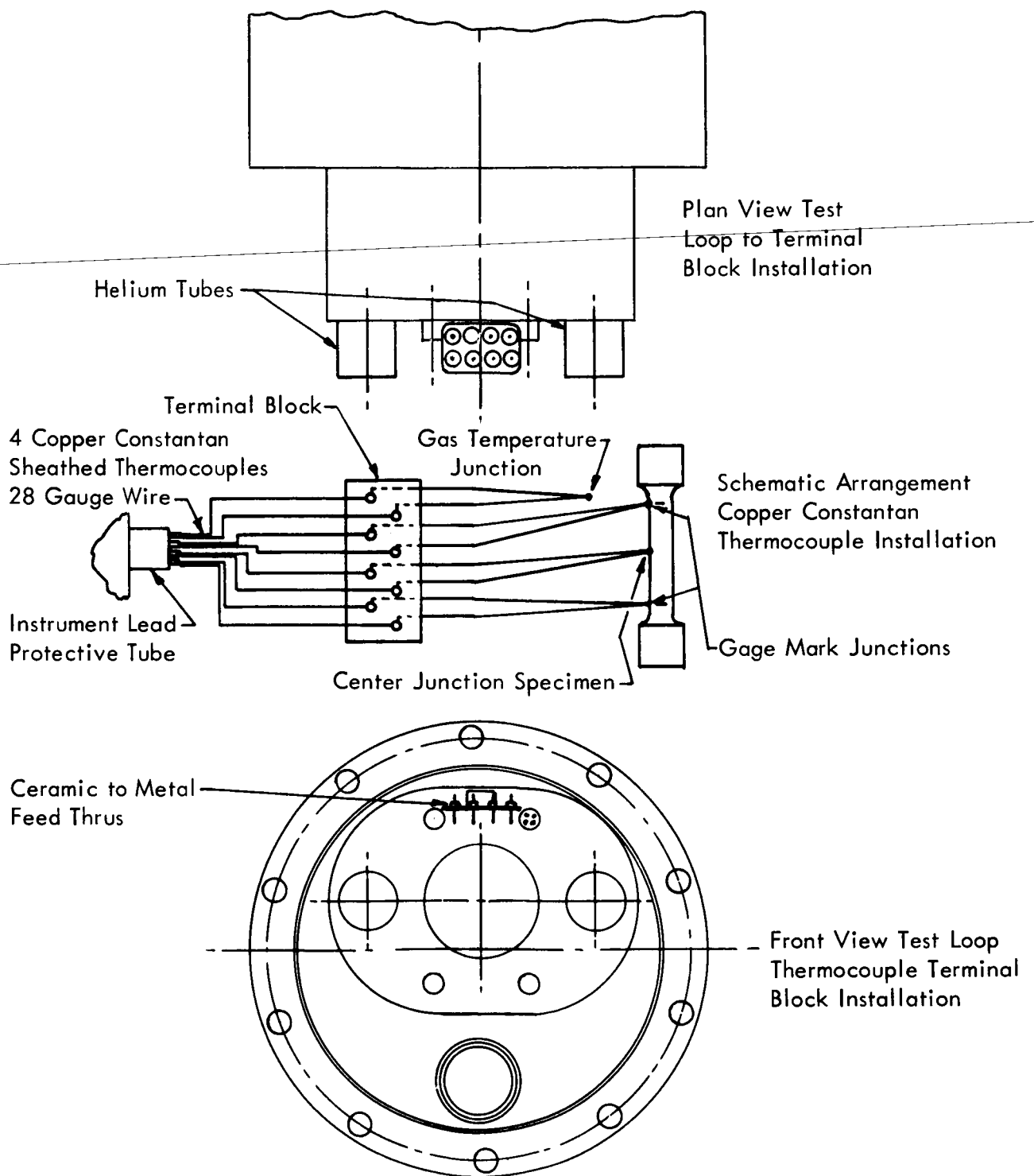


FIGURE 22 THERMOCOUPLE INSTALLATION IN TEST LOOP

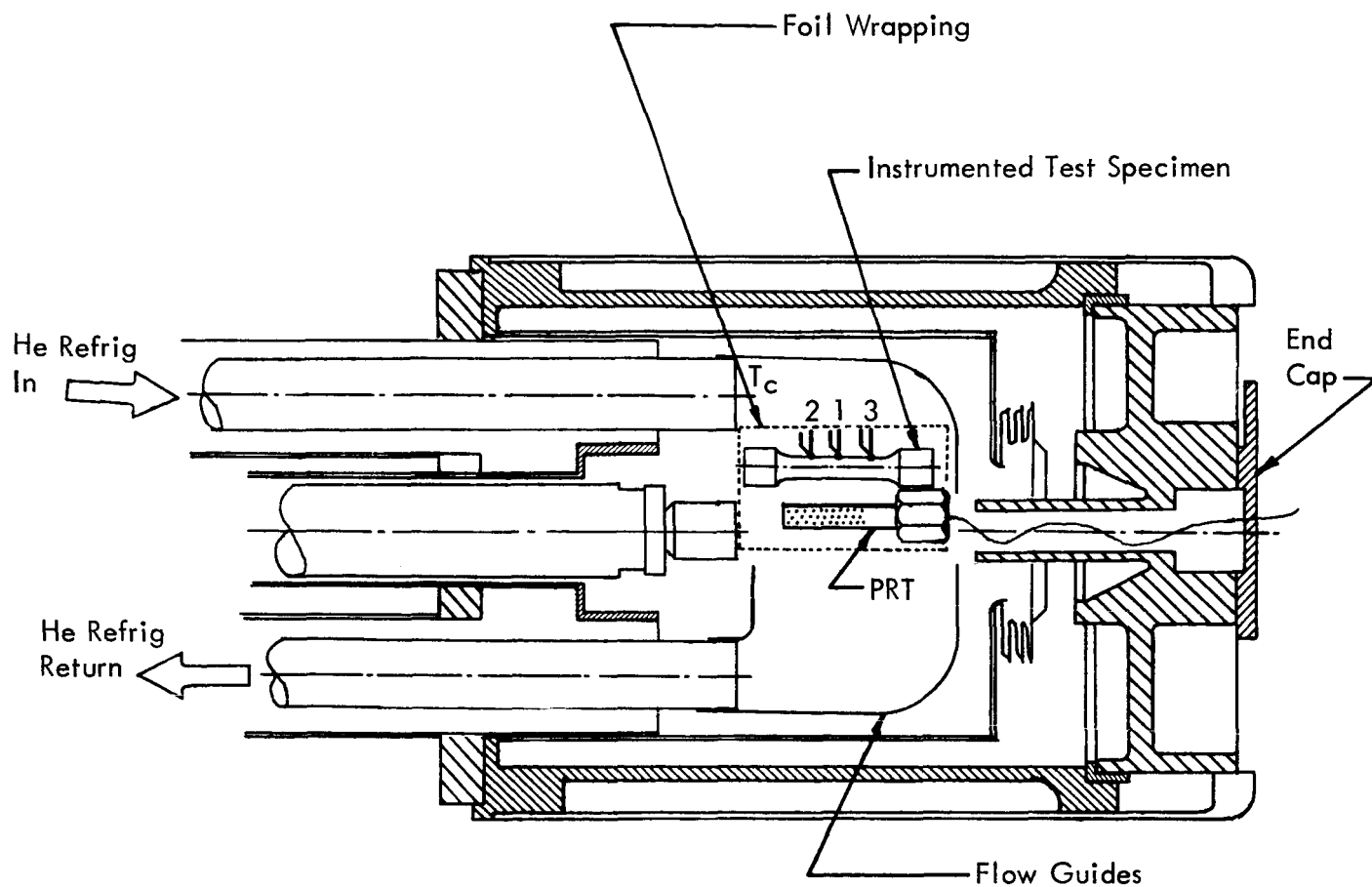


FIGURE 23 PLATINUM RESISTANCE THERMOMETER AND INSTRUMENTED SPECIMEN CALIBRATION ARRANGEMENT

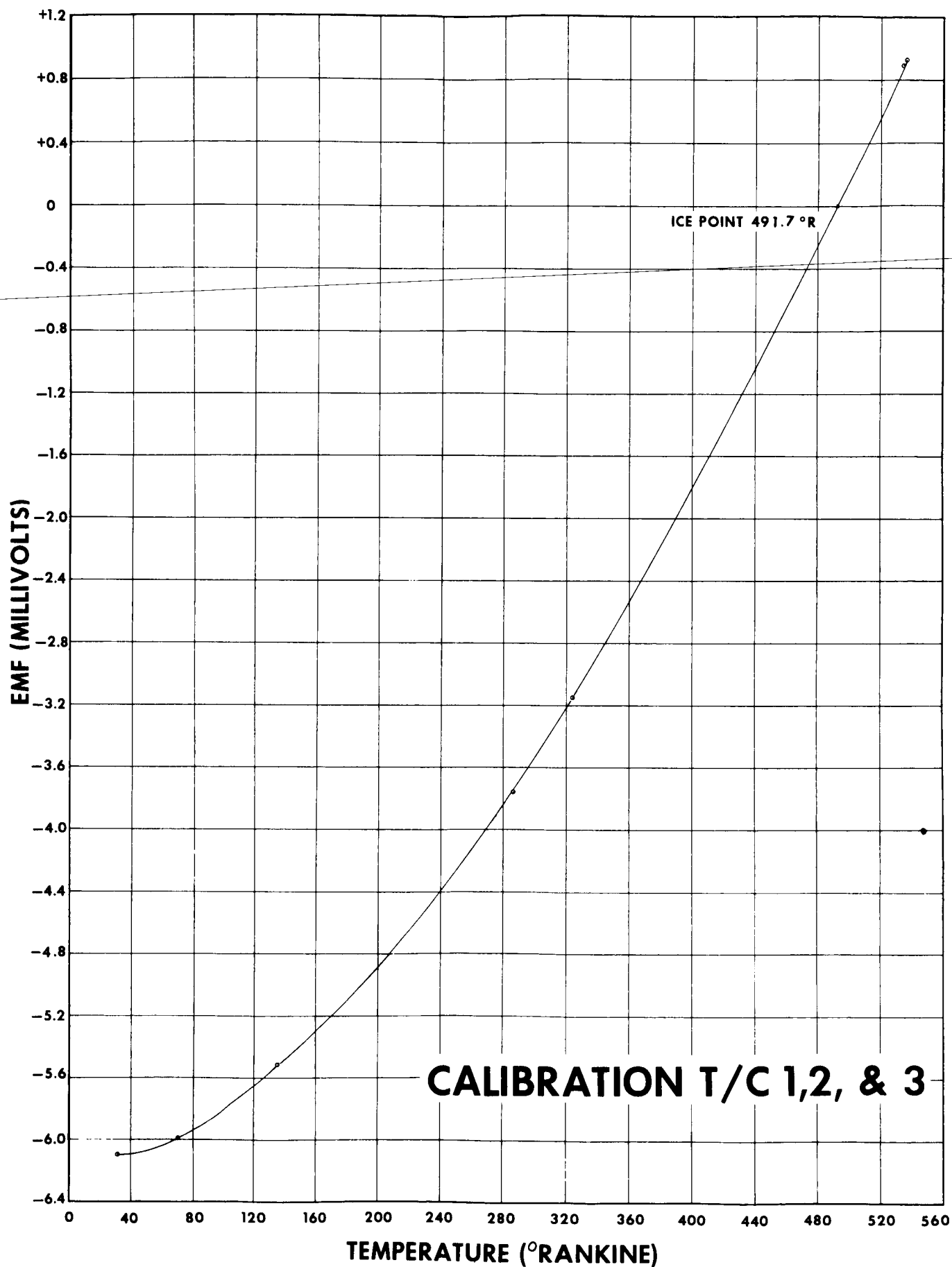


FIGURE 24 THERMOCOUPLE CALIBRATION CURVE

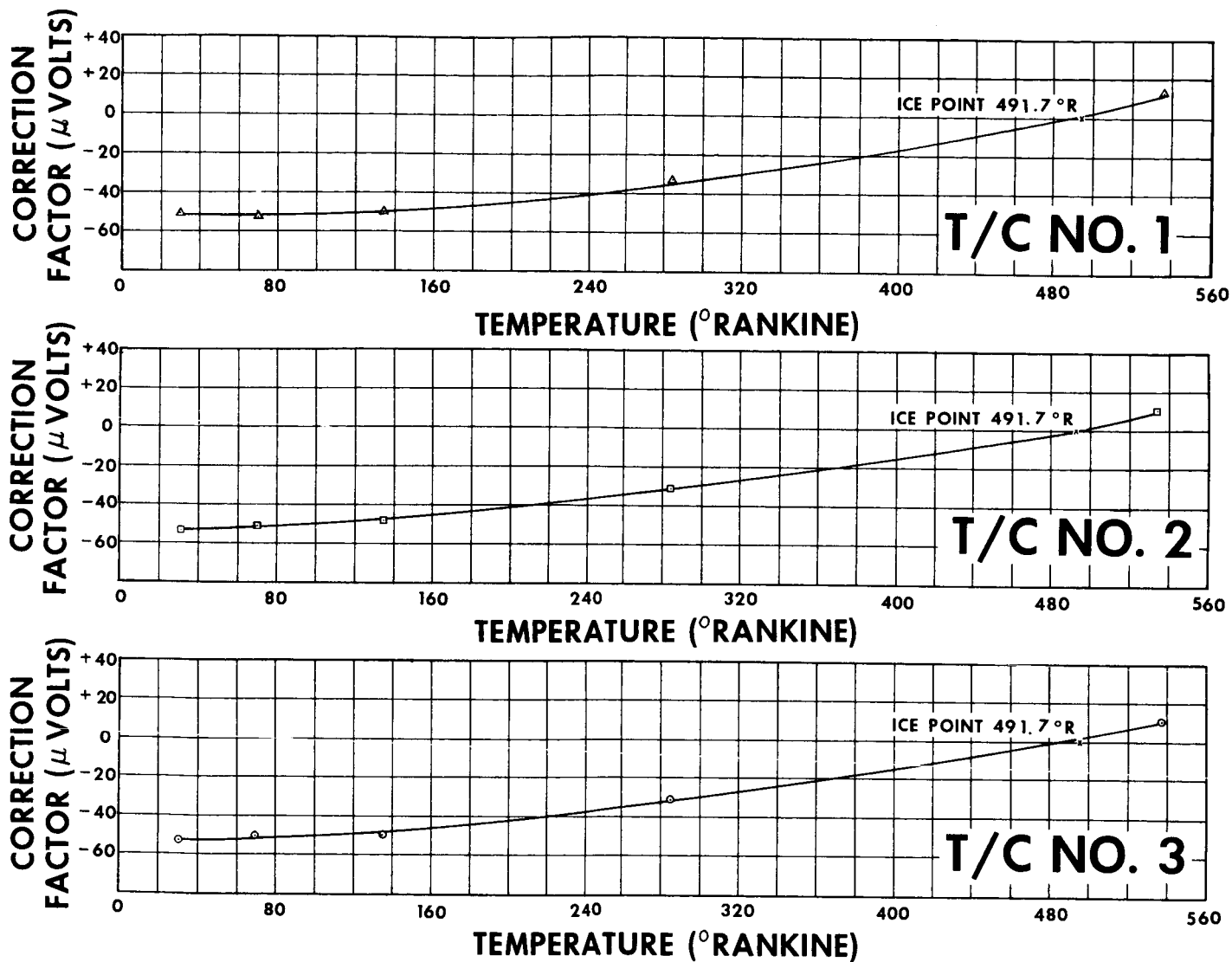


FIGURE 25 THERMOCOUPLE CORRECTION FACTORS

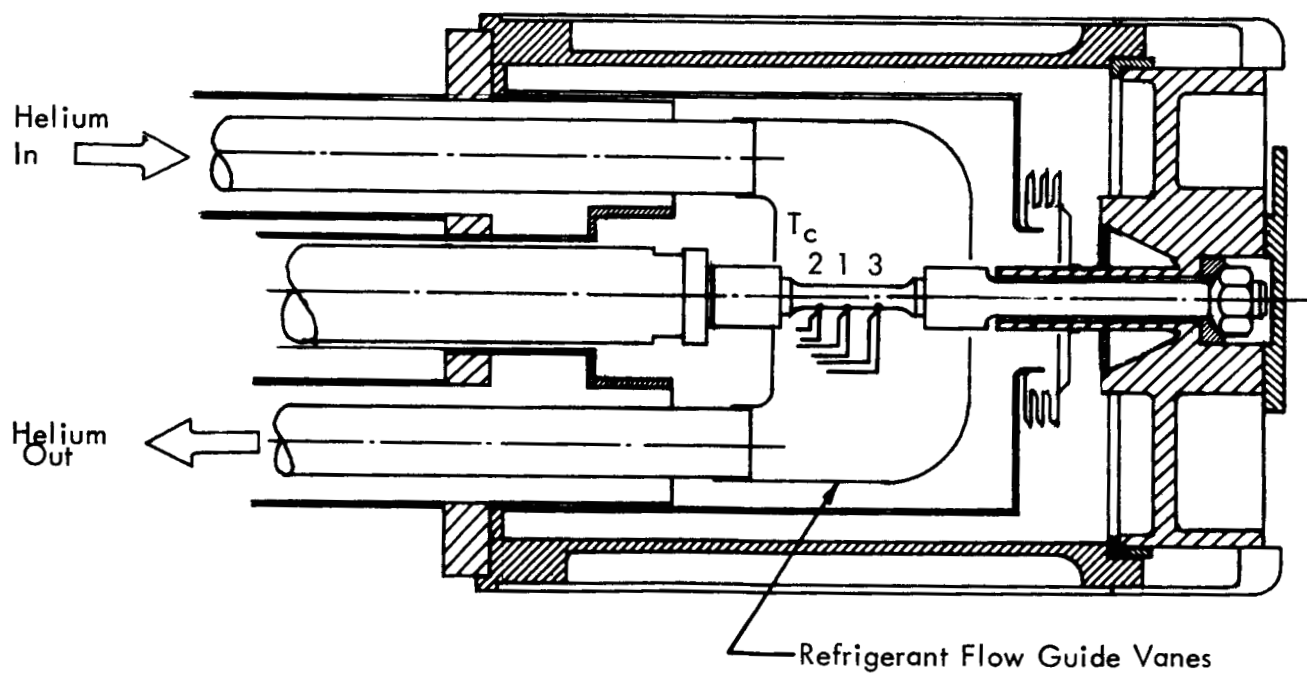


FIGURE 26 INSTRUMENTED SPECIMEN IN HOLDERS

All measurements were taken twice at the test point and each test point, or temperature, was repeated after measurements were taken at the next higher test temperature. Only one set of measurements was taken at 540°R due to a difficulty in maintaining refrigerator stability. The data obtained is currently being reduced for presentation in subsequent reports.

4.3.2 Strain Measurement

For tensile tests, the strain of unnotched tensile specimens is measured using an extensometer developed for this application. This extensometer measures the increase of the separation between two knife edges initially 0.50 inch apart. The measurement is accomplished through the use of a linear variable differential transformer (LVDT) specially constructed to be resistant to radiation effects.

The signal generated by the LVDT is read out on the X axis of a Moseley X-Y Recorder used to plot a load-strain curve for each specimen tested.

The extensometer was tested for reproducibility of signal at 30°R by repeatedly stressing an AISI 4130 steel test specimen to approximately 60% of its yield strength and comparing the modulus slope recorded for consistency.

The extensometers were verified and classified in accordance with ASTM Specification E-83 ⁽⁹⁾ using a Tuckerman optical strain gage as a primary standard. The error in indicated strain was less than 0.0001 in/in. This gives the extensometer an ASTM Classification of B-1, suitable for determination of modulus values as well as yield strength. However, this classification was obtained in a standards laboratory using precision techniques and this degree of accuracy cannot be expected following installation by remote means. As the extensometer is actually used, an ASTM Classification of B-2, suitable for determination of yield strength, but not of modulus, is probably a more realistic appraisal.

This extensometer has a range of reliable accuracy of approximately 0.010 in., or some 2% of the specimen gage length. This is sufficient to record the elastic portion of the load-strain curve and the initial plastic portion to well beyond the yield strength (0.2% offset method). However, the strain cannot be measured immediately prior to failure except for rather brittle materials. During plastic behaviour of the test specimen at strain levels beyond the capability of the extensometer, load is recorded against time of the X axis to provide a record of the

(9). Anon: ASTM Standards, Op. Cit.

loading pattern and to allow accurate determination of the fracture stress.

The strain rate, measured over 10 second intervals during the elastic behaviour of the test specimen, is approximately 0.0015 in/in/min. This method of measuring speed-of-testing conforms to ASTM E-8, paragraph 22.⁽¹⁰⁾

4.3.3 Load Measurement

The load applied to the test specimens in the tensile test loop is monitored by a proving ring type dynamometer using a linear variable differential transformer to measure the ring deflection resulting from loading. The transformer operates from a 2 kilocycle carrier oscillator and phase sensitive demodulator. The direct current output from this demodulator is fed through the X-Y Recorder where it is plotted on the Y axis as a direct measurement of stress.

Each dynamometer was calibrated prior to installation in the test loop by loading in series with a Morehouse vibrating reed proving ring calibrated by the National Bureau of Standards. The read out equipment associated with the test equipment was used to record dynamometer loading during calibration. The maximum difference in the load recorded by the dynamometer and the standard ring was less than 2%.

4.3.4 Data Recording

The temperature of the helium gas is monitored with platinum resistance thermometers located at the helium manifold on both the test loop inlet and return transfer lines. These control sensors are monitored by the test console operator and recorded on a specimen test log at regular intervals, which documents the proper control of the specimen temperature throughout the irradiation exposure.

The accumulated fast neutron flux dosage is calculated hourly. Both the incremental and accumulated flux are recorded in a data log to serve as a permanent record of the exposure received by each in-pile specimen.

For load-strain recording, the monitoring instruments convert load and strain into electrical signals proportional in strength to the magnitude of the load or strain being measured. The electrical impulse from each of these instruments is amplified

(10). Anon: ASTM Standards, Op. Cit.

and plotted automatically by a Moseley X-Y Recorder. Load appears as the Y plot, strain as the X plot and the resultant load-strain curves are recorded on graph paper as a permanent record of test data. The extensometer used in this program is capable of measuring only about 0.010 inch extension with reliable accuracy. After this limit of approximately 0.02 in/in total strain has been reached, the X axis recorder is switched to a time plot traveling at a rate of 0.02 in/sec.

The X-Y Recorder contains a calibrator which can provide a constant voltage of known amplitude to serve as a reference voltage. This calibration signal is continuously variable from 400 mv to 1400 mv and permits setting the X-Y Recorder range to conform with the individual calibrations of the extensometers and dynamometers.

The load-strain curve developed during testing by the X-Y Recorder and the initial specimen dimensions provide data for the determination of the ultimate tensile strength (F_{tU}) and the tensile yield strength (F_{ty}). The modulus of elasticity may be approximated from these curves, but an exact determination of this value is unobtainable due to the method of extensometer installation imposed by the necessity of using remote handling techniques.

4.3.5 Ductility Measurements

Elongation and reduction of area values were obtained by fitting the broken specimens together and measuring the fractured gage length and minimum diameter by means of a micrometer stage and hair line apparatus accurate to ± 0.0001 in. These values are reported as the change in magnitude from original specimen dimensions expressed as a percentage of the original value.

4.3.6 Data Reduction

As described previously, load-strain curves are plotted up to strains of approximately 2 percent and thereafter the load is plotted versus time until after failure of the specimen.

The load scale is varied to accommodate the approximate ultimate stress of the material being tested while the strain scale is held constant.

In nearly all measurements of tensile specimens, it is possible to estimate the slope of the so-called elastic portion of the load-strain curve and to thus determine a yield point corresponding to 0.2 percent plastic strain. This slope is also used to determine an approximate modulus of elasticity value.

The scale used and the yield increment are recorded on a master calculation sheet as are the ultimate load increment and the fracture load increment.

The elongated gage length and reduced diameter of the failed specimens are measured and these dimensions also are recorded on the master calculation sheet for the particular material.

4.4 FATIGUE TEST METHODS

After extensive modification of the test equipment, low-cycle fatigue characteristics of the selected materials will be studied. The fatigue testing portion of this program is divided into two experiments: cyclic load testing during irradiation at 30°R and cyclic load testing after irradiation to 10^{17} nvt ($E > 0.5$ Mev) at 30°R with appropriate control tests at 30°R and 540°R without irradiation.

4.4.1 Low-Cycle Fatigue During Irradiation

The test procedure will consist of applying a pre-determined stress load at a cyclic rate of 6 cpm for 10,000 cycles unless the test is interrupted before this point by specimen failure. The initial stress level will be 90% of the previously established ultimate tensile strength for the material at the given test condition; subsequent stress levels will be established on the basis of test results. The tests will be performed at 540°R and 30°R, unirradiated and at 30°R during irradiation with the initial load application made at the start of the irradiation period. A maximum of nine specimens for each material and condition will be performed in each of the experimental conditions. The test data will be reported as a plot of cycles to failure versus applied stress for each condition.

4.4.2 Low-Cycle Fatigue Following Irradiation to 10^{17} nvt

This phase of the test program is similar to that described above except that the irradiated specimens are subjected to an exposure of 1×10^{17} nvt ($E > 0.5$ Mev) at

30°R and withdrawn from the beam port prior to the initial load application. The cyclic load rate is again 6 cpm and the applied stress will be determined on the basis of initial testing at 90% of the ultimate strength for the material and test condition. As with the other testing, appropriate control tests without irradiation will be performed.

4.5 STRUCTURAL STUDIES

Structural studies will be performed with the aid of optical microscopy, electron microscopy, and X-ray diffraction. Procedures for these methods are being developed with the assistance of NASA Plum Brook Reactor Facility personnel and will be reported in later progress reports.

It is expected that transmission electron microscopy studies of the failed tensile specimens and electron fractographs of the fatigue specimens may be particularly valuable although both of these techniques present considerable difficulty, particularly in hot cell operations.

5 TEST PROGRAM

5.1 MATERIALS SELECTION

The materials, pure aluminum, titanium and titanium alloys, to be tested during this program were selected on the basis of their potential usefulness in nuclear-cryogenic space hardware and their ability to yield fundamental information in terms of basic mechanisms occurring in metals and alloys during and following fast neutron irradiation at cryogenic temperatures.

The titanium alloys of primary alpha structure usually exhibit good cryogenic properties due to the hexagonal close-packed structure of this phase. They have a high modulus of rigidity and a high strength-weight ratio which is comparable with the best aluminum alloys. Also, they have allowable working temperatures which are higher than the aluminum alloys. This makes them more suitable for rocket components since initially during rocket firing at cryogenic temperatures they may see elevated temperatures. Titanium-5% Al - 2.5% Sn with standard interstitial content and the same alloy with extra low interstitial content are to be tested along with Titanium - 6% Al - 4% V in both the annealed and aged conditions.

Titanium - 5% Al - 2.5% Sn is a fairly high strength alpha phase alloy ($F_{TU} \approx 120$ Ksi at room temperature). It is now commercially available in the extra low interstitial grade (less than 0.125% interstitials, and designated eli) and possibly would be specified in this grade by designers for use in shells, pressure vessels and pump parts of nuclear rockets. However, recent nuclear cryogenic tests to 10^{17} nvt ($E > 0.5$ Mev) at 30°R indicate that the ultimate strength of the eli material is adversely effected by the neutron irradiation. It is conceivable that higher irradiations might cause adverse effects on various properties, including fatigue strength, which would negate any inherent advantages of the eli material. In addition, tensile testing of both grades of this alloy might yield fundamental information on the general role of interstitials in nuclear cryogenic processes occurring in all metals and alloys.

Titanium - 6% Al - 4% V is an alpha-beta alloy in which the beta phase is metastable in the annealed condition and largely transformed to alpha by aging. The ultimate strength of the aged materials is about 170 ksi at room temperature with favorable cryogenic characteristics and it is very likely to be specified for shells and pressure vessels in space hardware. Irradiation to 10^{17} nvt at 30°R causes measurable increases in the strength of the aged material but not the annealed material. High irradiations at the same temperature may confirm this effect and may possibly yield fundamental information regarding the effects of nuclear irradiation on precipitation processes. Such effects are still not very well understood although they are of wide general interest to both basic researchers and applications people.

Titanium 55A, although of only moderate strength, has good forming characteristics and meets the requirements for some nuclear rocket applications; however, it was selected for study in this program primarily because it is essentially commercially pure elemental titanium and may yield important fundamental information. It has exhibited a small but measurable increase in yield strength due to fast neutron irradiation of 10^{17} nvt at 30°R.

Aluminum 1099 was selected for study because it has exhibited very large effects due to irradiation at 30°R as well as some annealing effects and effects due to deformation prior to irradiation. It is high purity aluminum and, of all the materials selected, offers the best opportunity for study of the fundamental irradiation mechanisms, although it is of little value as a structural material.

5.2 SCOPE

The test program, shown in Tables 1 and 2, consists of the following eight general areas of study:

- (1) Effect of irradiation at 30°R on tensile properties of pure aluminum (1099 Al).
- (2) Effect of irradiation temperature on tensile properties of pure aluminum (1099 Al).
- (3) Effect of annealing on tensile properties of pure aluminum (1099 Al) irradiated at 30°R.
- (4) Effect of irradiation at 30°R on tensile properties of titanium and titanium alloys.
- (5) Effect of irradiation at 30°R on low-cycle fatigue properties of titanium and titanium alloys.
- (6) Effect of irradiation at 30°R on low-cycle fatigue properties of pure aluminum (1099 Al).
- (7) Effect of cryogenic temperature on tensile properties of commercially pure titanium.
- (8) Effect of cryogenic temperature on tensile properties of 7178 Aluminum alloy.

TABLE 1 -- TENSILE TEST PROGRAM (SCOPE)

Material	Condition	Number Specimens	E x p o s u r e			Remarks
			n/cm ² (E>0.5 Mev)	Temperature (°R)		
				Exposure	Post-Exposure	
1099 Al	-H14	5	0	30	--	(1)
1099 Al	-H14	3	1 × 10 ¹⁷	30	--	(2)
1099 Al	-H14	3	3 × 10 ¹⁷	30	--	
1099 Al	-H14	3	0	140	--	
1099 Al	-H14	3	1 × 10 ¹⁷	140	--	
1099 Al	-H14	3	0	320	--	
1099 Al	-H14	3	1 × 10 ¹⁷	320	--	
1099 Al	-H14	5	0	540	--	(1)
1099 Al	-H14	3	1 × 10 ¹⁷	540	--	
1099 Al	-H14	3	0	30	140	(3)
1099 Al	-H14	3	1 × 10 ¹⁷	30	140	(4)
1099 Al	-H14	3	0	30	320	(3)
1099 Al	-H14	3	1 × 10 ¹⁷	30	320	(4)
1099 Al	-H14	3	0	30	540	(3)
1099 Al	-H14	3	1 × 10 ¹⁷	30	540	(4)
Ti-55A	Annealed	10	0	540	--	(5)
Ti-55A	Annealed	10	0	140	--	(5)
Ti-55A	Annealed	5	0	30	--	(1)
Ti-55A	Annealed	3	1 × 10 ¹⁷	30	--	(1)
Ti-55A	Annealed	3	6 × 10 ¹⁷	30	--	
Ti-55A	Annealed	3	1 × 10 ¹⁸	30	--	
Ti-5Al-2.5 Sn (ELI)	Annealed	5	0	540	--	(1)
"	Annealed	5	0	30	--	(1)
"	Annealed	3	1 × 10 ¹⁷	30	--	(1)
"	Annealed	3	1 × 10 ¹⁸	30	--	
Ti-5Al-2.5 Sn (STD)	Annealed	5	0	540	--	(1)
"	Annealed	5	0	30	--	(1)
"	Annealed	3	1 × 10 ¹⁷	30	--	(1)
"	Annealed	3	1 × 10 ¹⁸	30	--	
Ti-6Al-4V	Annealed	5	0	540	--	(1)
Ti-6Al-4V	Annealed	5	0	30	--	(1)
Ti-6Al-4V	Annealed	3	1 × 10 ¹⁷	30	--	(1)
Ti-6Al-4V	Annealed	3	1 × 10 ¹⁸	30	--	
Ti-6Al-4V	Aged	5	0	540	--	(1)
Ti-6Al-4V	Aged	5	0	30	--	(1)
Ti-6Al-4V	Aged	3	1 × 10 ¹⁷	30	--	(1)
Ti-6Al-4V	Aged	3	1 × 10 ¹⁸	30	--	
7178 Al		10	0	540	--	(5)
7178 Al		10	0	140	--	(5)

REMARKS:

- (1) Data available from screening program (Reference 1).
- (2) Some data also available from screening program (Reference 1).
- (3) To be held at exposure temperature for 14 hours.
- (4) To be fractured at post-exposure temperature.
- (5) Data for five specimens available from screening program (Reference 1).

TABLE 2 -- FATIGUE TEST PROGRAM (SCOPE)

Material	No. Specimens (Max)	Test Type	Exposure		
			°R	Cpm	Location
1099 Al	9	Fatigue During Exposure	540	6	Out-of-pile
1099 Al	9	Fatigue During Exposure	30	6	Out-of-pile
1099 Al	9	Fatigue During Exposure	30	6	In-pile
Ti-55A	9	Fatigue During Exposure	540	6	Out-of-pile
Ti-55A	9	Fatigue During Exposure	30	6	Out-of-pile
Ti-55A	9	Fatigue During Exposure	30	6	In-pile
Ti-5Al-2.5 Sn (Eli)	9	Fatigue During Exposure	540	6	Out-of-pile
Ti-5Al-2.5 Sn (Eli)	9	Fatigue During Exposure	30	6	In-pile
Ti-5Al-2.5 Sn (Eli)	9	Fatigue During Exposure	30	6	In-pile
Ti-5Al-2.5 Sn (Std)	9	Fatigue During Exposure	540	6	Out-of-pile
Ti-5Al-2.5 Sn (Std)	9	Fatigue During Exposure	30	6	Out-of-pile
Ti-5Al-2.5 Sn (Std)	9	Fatigue During Exposure	30	6	In-pile
Ti-6Al-4V (Ann)	9	Fatigue During Exposure	540	6	Out-of-pile
Ti-6Al-4V (Ann)	9	Fatigue During Exposure	30	6	Out-of-pile
Ti-6Al-4V (Ann)	9	Fatigue During Exposure	30	6	In-pile
Ti-6Al-4V (Aged)	9	Fatigue During Exposure	540	6	Out-of-pile
Ti-6Al-4V (Aged)	9	Fatigue During Exposure	30	6	Out-of-pile
Ti-6Al-4V (Aged)	9	Fatigue During Exposure	30	6	In-pile

Material	No. Specimens (Max)	Test Type	Exposures nvt(E>0.5 Mev)°R	Post-Exposure	
				°R	cpm
1099 Al	9	Post-Exposure Fatigue	0 30	30	6
1099 Al	9	Post-Exposure Fatigue	1 x 10 ¹⁷ (14 hr)	30	6
Ti-55A	9	Post-Exposure Fatigue	0 30	30	6
Ti-55A	9	Post-Exposure Fatigue	1 x 10 ¹⁷ 30	30	6
Ti-5Al-2.5 Sn (Eli)	9	Post-Exposure Fatigue	0 30	30	6
			(14 hr)		
Ti-5Al-2.5 Sn (Eli)	9	Post-Exposure Fatigue	1 x 10 ¹⁷ 30	30	6
Ti-5Al-2.5 Sn (Std)	9	Post-Exposure Fatigue	0 30	30	6
			(14 hr)		
Ti-5Al-2.5 Sn (Std)	9	Post-Exposure Fatigue	1 x 10 ¹⁷ 30	30	6
Ti-6Al-4V (Ann)	9	Post-Exposure Fatigue	0 30	30	6
			(14 hr)		
Ti-6Al-4V (Ann)	9	Post-Exposure Fatigue	1 x 10 ¹⁷ 30	30	6
Ti-6Al-4V (Aged)	9	Post-Exposure Fatigue	0 30	30	6
			(14 hr)		
Ti-6Al-4V (Aged)	9	Post-Exposure Fatigue	1 x 10 ¹⁷ 30	30	6

As noted on Table 1, data obtained from the screening program⁽¹⁾ is to be included in the analysis of the effects of irradiation at cryogenic temperatures on materials. Complimentating the mechanical property tests will be the structural studies, also using data obtained from the screening program for analysis.

(1). Quarterly Progress Reports 1-16, Contract NASw-114.

APPENDIX A
DISTRIBUTION

National Aeronautics & Space
Administration
Space Nuclear Propulsion
Office-Cleveland
Lewis Research Center
21000 Brookpark Road
Cleveland, Ohio 44135
Attention: L. C. Corrington

National Aeronautics & Space
Administration
Washington, D. C. 20546
Attention: George C. Deutsch
(Code RRM)

NASA-Lewis Research Center
21000 Brookpark Road
Cleveland, Ohio 44135
Attention: M.H. Krasner

AEC-NASA Space Nuclear
Propulsion Office
U. S. Atomic Energy Commission
Washington, D. C. 20545
Attention: Harold B. Finger,
Manager

NASA-Scientific & Technical
Information Facility
Box 5700
Bethesda, Maryland 20014
Attention: NASA Representative
(CRT)

NASA-Lewis Research Center
21000 Brookpark Road
Cleveland, Ohio 44135
Attention: Library

AEC-NASA Space Nuclear
Propulsion Office
U.S. Atomic Energy Commission
Washington, D.C. 20545
Attention: F. C. Schwenk

AEC-NASA Space Nuclear
Propulsion Office
U.S. Atomic Energy Commission
Washington, D.C. 20545
Attention: J.E. Morrissey

National Aeronautics & Space
Administration
Washington, D.C. 20546
Attention: David Novik, Chief
(Code RNV)

NASA-Lewis Research Center
21000 Brookpark Road
Cleveland, Ohio 44135
Attention: Charles L. Younger(NRD)

NASA-Lewis Research Center
21000 Brookpark Road
Cleveland, Ohio 44135
Attention: H.J. Heppler, Jr.

NASA-Plum Brook Station
Sandusky, Ohio 44871
Attention: Donald B. Crandall

NASA-Lewis Research Center
21000 Brookpark Road
Cleveland, Ohio 44135
Attention: Dr. John C. Liwosz

NASA-Lewis Research Center
21000 Brookpark Road
Cleveland, Ohio 44135
Attention: T.J. Flanagan (P&SD)

NASA-Langley Research Center
Langley Station
Hampton, Virginia 23365
Attention: Library

NASA-Lewis Research Center
21000 Brookpark Road
Cleveland, Ohio 44135
Attention: Norman T. Musial

NASA-Manned Spacecraft Center
Houston, Texas 77001
Attention: Library

NASA-Lewis Research Center
21000 Brookpark Road
Cleveland, Ohio 44135
Attention: Report Control Office

NASA-Western Operations
150 Pico Boulevard
Santa Monica, California 90406
Attention: Library

U.S. Atomic Energy Commission
Technical Reports Library
Washington, D.C.

U.S. Naval Research Laboratory
Washington, D.C. 20390
Attention: L.E. Steele, Head,
Reactor Materials Branch,
Metallurgy Division

NASA-Lewis Research Center
21000 Brookpark Road
Cleveland, Ohio 44135
Attention: Office of Reliability &
Quality Assurance

University of California
Los Alamos Scientific Laboratory
P.O. Box 1663
Los Alamos, New Mexico 87544
Attention: W.L. Kirk

NASA-Ames Research Center
Moffett Field, California 94035
Attention: Library

Lockheed Nuclear Products
Lockheed-Georgia Company
Information Center
Dawsonville, Georgia

NASA-Flight Research Center
P.O. Box 273
Edwards, California 93523
Attention: Library

William House
NERVA Project Manager
Aerojet-General Corporation
P.O. Box 296
Azusa, California

NASA-Goddard Space Flight Center
Greenbelt, Maryland 20771
Attention: Library

Aerojet-General Nucleonics
A Div. of Aerojet-General Corp.
P.O. Box 77
San Ramon, California 94583
Attention: G.A. Linenberger,
General Manager

Jet Propulsion Laboratory
4800 Oak Grove Drive
Pasadena, California 91103
Attention: Library

Aerojet General Corporation
NERVA Operations
P.O. Box 296
Azusa, California
Attention: C.N. Trent,
Associate Director

Aluminum Company of America
P.O. Box 1012
New Kensington, Pennsylvania
Attention: Edwin H. Spuhler

Argonne National Laboratories
P.O. Box 299
Lemont, Illinois
Attention: T.H. Blewitt

Argonne National Laboratory
Library Services Dept. 203-CE125
9700 South Cass Avenue
Argonne, Illinois 60440
Attention: Report Section

IIT Research Institute
10 W. 35th Street
Chicago 16, Illinois
Attention: D.J. McPherson,
Vice President

Battelle Memorial Institute
Radiation Effects Information Center
505 King Avenue
Columbus, Ohio 43201
Attention: D.J. Hamman

Battelle Memorial Institute
Columbus 1, Ohio
Attention: Roger J. Runck

Beech Aircraft Corporation
P.O. Box 631
Boulder, Colorado 80301
Attention: Technical Library

The Boeing Company
Aerospace Group
P.O. Box 3707
Seattle, Washington 98124
Attention: Ruth E. Peerenboom,
Processes Supervisor

Brookhaven National Laboratory
Department of Physics
Upton Long Island, New York 11973
Attention: Paul W. Levy

California Institute of Technology
General Library
1201 East California Street
Pasadena, California 91109

Lawrence Radiation Laboratory
University of California
Technical Information Division
Berkeley, California

University of California
Engineering & Mathematical
Sciences Library
405 Hilgard Avenue
Los Angeles, California 90024

Carbone Company
Toonton, New Jersey
Attention: E.P. Eaton

Carpenter Steel Company
P.O. Box 662
Reading, Pennsylvania
Attention: Neil J. Culp

Institute of Metals Library
University of Chicago
5640 Ellis
Chicago, Illinois 60637

University of Colorado
Engineering Research Center
Boulder, Colorado
Attention: K.D. Timmerhaus,
Associate Dean of Engineering

Fort Worth Division of
General Dynamics
P.O. Box 748
Fort Worth, Texas 76101
Attention: Bob Vollmer,
Administrative Assistant

Picatinny Arsenal
Technical Information Section
Dover, New Jersey 07801
Attention: Commanding Officer
SMUPA-VA6

General Electric Company
Nuclear Materials & Propulsion
Operation
P.O. Box 132
Cincinnati, Ohio 45215
Attention: J. W. Stephenson

University of Georgia Libraries
Acquisitions Division
Athens, Georgia 30601

Huntington Alloy Products Division
International Nickel Company, Inc.
Huntington 17, West Virginia
Attention: E. B. Fernsler

Lawrence Radiation Laboratory
Technical Information Division
University of California
P.O. Box 808
Livermore, California

Arthur D. Little Co., Inc.
Acorn Park
Cambridge, Massachusetts
Attention: Charles A. Schulte

Lockheed-California Company
Burbank, California 91503
Attention: Dr. Lewis Larmore,
Chief Scientist

Lockheed-California Company
Central Library, Bldg. 63
Scientific and Technical Information
Center
Burbank, California

Lockheed-California Company
Engineering Research
Burbank, California
Attention: H. B. Wiley

Lockheed Missiles & Space Company
Materials Research Staff
3251 Hanover Street
Palo Alto, California
Attention: John C. McDonald

Lockheed Missiles & Space Company
Nuclear Space Programs
Sunnyvale, California
Attention: H.F. Plank

Lockheed Missiles & Space Company
Sci-Tech Information Center
Palo Alto, California

Lockheed Missiles & Space Company
3251 Hanover Street
Palo Alto, California
Attention: M.A. Steinberg, 52-30,201

Los Alamos Scientific Laboratory
Report Library
P.O. Box 1663
Los Alamos, New Mexico 87544

George C. Marshall Space Flight
Center
Huntsville, Alabama
Attention: W.Y. Jordan, P&VE-FN

George C. Marshall Space Flight
Center
Huntsville, Alabama 35812
Attention: Dr. W. R. Lucas,
M-P & VE-M

George C. Marshall Space Flight
Center
Huntsville, Alabama 35812
Attention: R.D. Shelton, M-RP-N

The Martin Company
P.O. Box 179
Denver, Colorado 80201
Attention: F. R. Schwartzberg,
G0534

University of Michigan
University Library
Ann Arbor, Michigan 48104
Attention: Robert G. Carter

Atomics International
P.O. Box 309
Canoga Park, California
Attention: F.E. Farhat, Librarian

Northrop Corporation
Norair Division
3901 W. Broadway
Hawthorne, California
Attention: Technical Information,
3343-32

Oak Ridge National Laboratory
Oak Ridge, Tennessee 37831
Attention: D.S. Billington

U.S. Atomic Energy Commission
Division of Technical Information
Extension
P.O. Box 62
Oak Ridge, Tennessee 37831

Purdue University
Lafayette, Indiana
Attention: Librarian

Pennsylvania State University
Engineering Mechanics Department
105 Hammond Building
University Park, Pennsylvania 16802
Attention: Mr. Joseph Marin

Pure Carbon Company
Wellsville Street
Saint Marys, Pennsylvania
Attention: Robert Paxon

Reynolds Metals Company
6601 West Broad Street
Richmond, Virginia
Attention: L.E. Householder

Rice University
The Fondren Library
P.O. Box 1892
Houston, Texas 77001

Southeastern Research Institute
Birmingham, Alabama
Attention: J.R. Kattus

Special Metals, Inc.
New Hartford, New York
Attention: Robert Neilsen

TRW Systems
Technical Information Center
One Space Park
Redondo Beach, California

Air Force Weapons Laboratory
Kirtland AFB, New Mexico 87117
Attention: Technical Library (WLIL)

National Bureau of Standards
Cryogenic Data Center
Boulder, Colorado 80302

National Bureau of Standards
U.S. Department of Commerce
Cryogenic Engineering Laboratory
Boulder, Colorado
Attention: R.P. Reed

Bureau of Naval Weapons
Washington 25, D.C.
Attention: Captain J.H. Terry,
RRNU

U.S. Naval Research Laboratory
Mechanics Division
Code 6204
Washington, D.C. 20390
Attention: Dr. Albert V.H. Masket

United States Steel Corporation
Monroeville, Pennsylvania
Attention: Waldo Rall

Watertown Arsenal
U.S. Army Materials Research Agency
Watertown, Massachusetts
Attention: T.S. DeSisto

Westinghouse Electric Corporation
Metallurgical Division, Research &
Development Center
Pittsburgh, Pennsylvania 15235
Attention: E. T. Wessel

Westinghouse Astronuclear Laboratory
Materials Department
P.O. Box 10864
Pittsburgh 36, Pennsylvania
Attention: Dr. D.E. Thomas, Manager

AFML (MAAM) (1A)
Wright-Patterson AFB, Ohio 45433

Wright-Patterson Air Force Base
Foreign Technology Division
TDEPR
Dayton, Ohio
Attention: Lt. Schauffle, USAF

Titanium Metals Corporation of America
233 Broadway
New York City, New York
Attention: E.F. Erbin, Staff

Lockheed-Georgia Company
P.O. Box 2155
Sandusky, Ohio 44871
Attention: C. A. Schwanbeck

Hughes Aircraft Company
Nucleonics Division
Fullerton, California
Attention: Dr. A.M. Liebschutz

Lockheed-Georgia Company
Nuclear Laboratories
Dawsonville, Georgia
Attention: Dr. M.M. Miller, Manager
Nuclear Aerospace Division

AF Materials Laboratory
Research & Technology Division
AFSC
Wright-Patterson AFB, Ohio 45433
Attention: Harold M. Hormann

University of California
University Research Library
Los Angeles, California 90024
Attention: Serials Department

Kaman Aircraft Corporation
Kaman Nuclear Division
Colorado Springs, Colorado
Attention: Mary G. Brown,
Librarian

North American Aviation
Rocketdyne Division
6633 Canoga Avenue
Canoga Park, California
Attention: Technical Information
Center

Sandia Corporation
Sandia Base
P.O. Box 5800
Albuquerque, New Mexico 87115
Attention: Technical Library

General Dynamics Convair
Materials & Processes Section
P.O. Box 1128
San Diego, California 92112
Attention: A. Hurlich, Manager
Mail Zone 572-00

Battelle-Northwest
Post Office Box 999
Richland, Washington
Attention: Spencer H. Bush

Brookhaven National Laboratory
Upton Long Island, New York 11973
Attention: D.H. Gurinsky

Department of the Army
United States Army Munitions
Command
Frankford Arsenal
Philadelphia 37, Pennsylvania
Attention: Librarian

Rocketdyne
Division of North American
Aviation, Inc.
6633 Canoga Avenue
Canoga Park, California
Attention: G.A. Fairbairn,
D/596-174, Z-2

Los Alamos Scientific Laboratory
Los Alamos, New Mexico 87544
Attention: Glen A. Graves

Bendix Corporation
Research Laboratory Division
Library Services
Southfield, Michigan
Attn: Frank W. Poblentz

Douglas Aircraft Company, Inc.
Missile & Space Systems Division
3000 Ocean Park Blvd.
Santa Monica, California 90406
Attention: A2-260 Library

ABSTRACT

This is the first quarterly report for a study of the effect of nuclear radiation on materials at cryogenic temperatures. These studies include the effect of:

- (1) 10^{18} n/cm² at 30°R on tensile properties of titanium-base alloys;
- (2) irradiation temperature (30°R to 540°R) on tensile properties of 1099-H14 Aluminum following irradiations up to 3×10^{17} n/cm²;
- (3) annealing following irradiation at 30°R to 10^{17} n/cm² on tensile properties of 1099-H14 Aluminum;
- and (4) irradiation at 30°R on axial, low-cycle fatigue properties of titanium-base alloys.

This report describes modifications to existing test equipment, maintenance and calibration procedures, and introduces the test program.